

Anisotropic weakly over-penalised symmetric interior penalty method for the Stokes equation

Hiroki Ishizaka

Received: date / Accepted: date

Abstract In this study, we investigate an anisotropic weakly over-penalised symmetric interior penalty method for the Stokes equation on convex domains. Our approach is a simple discontinuous Galerkin method similar to the Crouzeix–Raviart finite element method. As our primary contribution, we show a new proof for the consistency term, which allows us to obtain an estimate of the anisotropic consistency error. The key idea of the proof is to apply the relation between the Raviart–Thomas finite element space and a discontinuous space. While inf-sup stable schemes of the discontinuous Galerkin method on shape-regular mesh partitions have been widely discussed, our results show that the Stokes element satisfies the inf-sup condition on anisotropic meshes. Furthermore, we also provide an error estimate in an energy norm on anisotropic meshes. In numerical experiments, we compare calculation results for standard and anisotropic mesh partitions.

Keywords Stokes equation · WOPSIP method · CR finite element method · RT finite element method · Anisotropic meshes

Mathematics Subject Classification (2010) 65D05 · 65N30

1 Introduction

In this study, we investigate a weakly over-penalised symmetric interior penalty (WOPSIP) method for the Stokes equations on anisotropic meshes. Brenner et al. first proposed a WOPSIP method [15], and several further works have considered similar techniques [8, 14, 16]. WOPSIP methods have two main advantages compared to standard symmetric interior penalty discontinuous Galerkin

Hiroki Ishizaka
Team fem, Matsuyama, Japan
E-mail: h.ishizaka005@gmail.com

(dG) methods [45, 47]. The first is that they are stable for any penalty parameter. Moreover, they work on nonconforming mesh partitions. Meanwhile, the drawback of the standard symmetric interior penalty discontinuous Galerkin method is that it requires tuning the penalty parameter for stability. Moreover, applying nonconforming meshes can be difficult in the classical Crouzeix–Raviart (CR) nonconforming finite element method ([19]). In the present work, we explore an error analysis on conformal meshes for simplicity. We briefly consider the case of nonconforming meshes in Section 5. The WOPSIP method is similar to the classical CR finite element method and thus has similar features such as inf-sup stability on anisotropic meshes. However, several studies have imposed the condition of shape regularity to a family of meshes, i.e., triangles or tetrahedra cannot be overly flat in a shape-regular family of triangulations.

Meanwhile, anisotropic meshes are effective for problems in which the solution has anisotropic behaviour in some direction of the domain. The anisotropic meshes do not satisfy the shape-regular condition or include elements with large aspect ratios. Given this background, several anisotropic finite element methods have been developed in recent years. [1, 2, 5, 6, 32, 33, 34, 35, 37, 36]. These methods aim to obtain optimal error estimates under the *semi-regular condition* defined in Assumption 1 [34] or the *maximum-angle condition*, which allows us to use anisotropic meshes; see Babuška et al. [7] for two-dimensional and Křížek’s work [40] three-dimensional cases. In this study, we consider the anisotropic WOPSIP method for the Stokes equation and present optimal error estimates in the energy norm.

The WOPSIP method is nonconforming. Therefore, an error between the exact and WOPSIP finite element approximation solutions for the velocity with an energy norm and the pressure with the L^2 -norm is divided into two parts. One part is an optimal approximation error in discontinuous finite element spaces, and the other is a consistency error term. For the former, the first-order CR interpolation errors (Theorem 3) and the error estimate of the L^2 -projection (Theorem 2) are used. However, estimating the consistency error term on anisotropic meshes is challenging. Barker and Brenner [8] apply the trace theorem when $d = 2$. Therefore, the shape regularity condition on meshes may be unavoidable with their proposed technique [8]. To overcome this difficulty, we use the relation between the lowest order Raviart–Thomas (RT) finite element interpolation and the discontinuous space; see Lemma 3. This relation derives an optimal error estimate of the consistency error (Lemma 9).

The remainder of this study is organised as follows. In Section 2, we introduce the (scaled) Stokes equation with the Dirichlet boundary condition, its weak formulation, and finite element settings for the WOPSIP method. In Section 3, we present the proposed WOPSIP approximation for the continuous problem and discuss its stability and error estimates. In Section 4, we provide the results of a numerical evaluation. Finally, we conclude by noting some limitations of the present work and suggesting some possible avenues for future research in Section 5. Throughout, we denote by c a constant independent of h (defined later) and of the angles and aspect ratios of simplices unless specified otherwise, and all constants c are bounded if the maximum angle is bounded.

These values may change in each context. The notation \mathbb{R}_+ denotes the set of positive real numbers.

2 Preliminaries

2.1 Weak formulation

We consider the following problem. Let $\Omega \subset \mathbb{R}^d$, $d \in \{2, 3\}$ be a bounded polyhedral domain. Furthermore, we assume that Ω is convex if necessary. The (scaled) Stokes problem is to find $(u, p) : \Omega \rightarrow \mathbb{R}^d \times \mathbb{R}$ such that

$$-\nu \Delta u + \nabla p = f \quad \text{in } \Omega, \quad \operatorname{div} u = 0 \quad \text{in } \Omega, \quad u = 0 \quad \text{on } \partial\Omega, \quad (2.1)$$

where ν is a nonnegative parameter and $f : \Omega \rightarrow \mathbb{R}^d$ is a given function.

To deduce a weak form of the continuous problem (2.1), we consider function spaces described as follows.

$$V := H_0^1(\Omega)^d, \quad Q := L_0^2(\Omega) := \left\{ q \in L^2(\Omega); \int_{\Omega} q dx = 0 \right\},$$

with norms:

$$|\cdot|_V := |\cdot|_{H^1(\Omega)^d}, \quad \|\cdot\|_Q := \|\cdot\|_{L^2(\Omega)}.$$

The variational formulation for the Stokes equations (2.1) is as follows. For any $f \in L^2(\Omega)^d$, find $(u, p) \in V \times Q$ such that

$$\nu a(u, \varphi) + b(\varphi, p) = \int_{\Omega} f \cdot \varphi dx \quad \forall \varphi \in V, \quad (2.2a)$$

$$b(u, q) = 0 \quad \forall q \in Q. \quad (2.2b)$$

Here, $a : H^1(\Omega)^d \times H^1(\Omega)^d \rightarrow \mathbb{R}$ and $b : H^1(\Omega)^d \times L^2(\Omega) \rightarrow \mathbb{R}$ respectively denote bilinear forms defined by

$$a(v, \psi) := \int_{\Omega} \nabla v : \nabla \psi dx = \sum_{i=1}^d \int_{\Omega} \nabla v_i \cdot \nabla \psi_i dx, \quad b(\psi, q) := - \int_{\Omega} \operatorname{div} \psi q dx.$$

Here, the colon denotes the scalar product of tensors.

Using the space of weakly divergence-free functions $V_{\sigma} := \{v \in V; b(v, q) = 0 \quad \forall q \in Q\}$, the associated problem to (2.2) is then to find $u \in V_{\sigma}$ such that

$$\nu a(u, \varphi) = \int_{\Omega} f \cdot \varphi dx \quad \forall \varphi \in V_{\sigma}. \quad (2.3)$$

The continuous inf-sup inequality

$$\inf_{q \in Q} \sup_{\psi \in V} \frac{b(\psi, q)}{|\psi|_V \|q\|_Q} \geq \beta > 0 \quad (2.4)$$

has been shown to hold. Proofs can be found in John [38, Theorem 3.46], Ern and Guermond [24, Lemma 53.9], and Girault and Raviart [27, Lemma 4.1].

We set

$$H_*^1(\Omega) := H^1(\Omega) \cap L_0^2(\Omega), \quad \mathcal{H} := \{v \in L^2(\Omega)^d : \operatorname{div} v = 0, v|_{\partial\Omega} \cdot n = 0\},$$

where $\operatorname{div} v = 0$ and $v|_{\partial\Omega} \cdot n = 0$ mean that $\int_{\Omega} (v \cdot \nabla) q dx = 0$ for any $q \in H_*^1(\Omega)$. Then, the following L^2 -orthogonal decomposition holds.

$$L^2(\Omega)^d = \mathcal{H} \oplus \nabla(H_*^1(\Omega)), \quad (2.5)$$

see [25, Lemma 74.1]. The L^2 -orthogonal projection $P_{\mathcal{H}} : L^2(\Omega)^d \rightarrow \mathcal{H}$ resulting from this decomposition is often called the *Leray projection*.

Theorem 1 (Stability) *For any $f \in L^2(\Omega)^d$ or $f \in V'$, the weak formulation (2.2) of the Stokes problem is well-posed. Furthermore, if $f \in V'$,*

$$|u|_V \leq \frac{1}{\nu} \|f\|_{V'}, \quad \|p\|_Q \leq \frac{2}{\beta} \|f\|_{V'}. \quad (2.6)$$

If $f \in L^2(\Omega)^d$,

$$|u|_V \leq \frac{c}{\nu} \|P_{\mathcal{H}}(f)\|_{L^2(\Omega)^d}, \quad \|p\|_Q \leq \frac{c}{\beta} \|f\|_{L^2(\Omega)^d}. \quad (2.7)$$

Proof A proof was provided by John [38, Theorem 4.6, Lemma 4.7]. \square

2.2 Trace inequality

The following trace inequality on anisotropic meshes is significant in this study. Some references can be found for the proof. Here, we follow Ern and Guermond [23, Lemma 12.15], also see Andreas [4, Lemma 2.3] and Kunnert [41, Lemma 2.2]. We note that although Lemma 12.15 in [23] imposes a shape-regular mesh condition, the condition is easily violated. For a simplex $T \subset \mathbb{R}^d$, let \mathcal{F}_T be the collection of the faces of T . Let $|\cdot|_d$ denote the d -dimensional Hausdorff measure.

Lemma 1 (Trace inequality) *Let $T \subset \mathbb{R}^d$ be a simplex. There exists a positive constant c such that for any $v = (v^{(1)}, \dots, v^{(d)})^T \in H^1(T)^d$, $F \in \mathcal{F}_T$, and h ,*

$$\|v\|_{L^2(F)^d} \leq c \ell_{T,F}^{-\frac{1}{2}} \left(\|v\|_{L^2(T)^d} + h_T^{\frac{1}{2}} \|v\|_{L^2(T)^d}^{\frac{1}{2}} |v|_{H^1(T)^d}^{\frac{1}{2}} \right), \quad (2.8)$$

where $\ell_{T,F} := \frac{d!|T|_d}{|F|_{d-1}}$ denotes the distance of the vertex of T opposite to F to the face.

Proof Let $v = (v^{(1)}, \dots, v^{(d)})^T \in H^1(T)^d$. Let P_F be the vertex of T opposite to F . By the same argument for $p = 2$ of [23, Lemma 12.15], together with the fact that $|x - P_F| \leq h_T$ and $\frac{|F|^{d-1}}{|T|^d} = \frac{d!}{\ell_{T,F}}$, it holds that for $i \in \{1, \dots, d\}$,

$$\|v^{(i)}\|_{L^2(F)}^2 \leq \frac{d!}{\ell_{T,F}} \|v^{(i)}\|_{L^2(T)}^2 + \frac{2(d-1)!}{\ell_{T,F}} h_T \|v^{(i)}\|_{L^2(T)} \|\nabla v^{(i)}\|_{L^2(T)^d}.$$

Using the Cauchy–Schwarz inequality, we obtain the target inequality together with the Jensen’s inequality. \square

Remark 1 Because $|T|_d \approx h_T^d$ and $|F|_{d-1} \approx h_T^{d-1}$ on the shape-regular mesh, it holds that $\ell_{T,F} \approx h_T$. Then, the trace inequality (2.8) is given as

$$\|v\|_{L^2(F)^d} \leq ch_T^{-\frac{1}{2}} \left(\|v\|_{L^2(T)^d} + h_T^{\frac{1}{2}} \|v\|_{L^2(T)^d} |v|_{H^1(T)^d}^{\frac{1}{2}} \right).$$

2.3 Meshes, mesh faces, averages and jumps

For simplicity, we consider conformal meshes. Let $\Omega \subset \mathbb{R}^d$ be a bounded polyhedral domain. Let $\mathbb{T}_h = \{T\}$ be a simplicial mesh of $\overline{\Omega}$ made up of closed d -simplices such as

$$\overline{\Omega} = \bigcup_{T \in \mathbb{T}_h} T,$$

with $h := \max_{T \in \mathbb{T}_h} h_T$, where $h_T := \text{diam}(T)$. For simplicity, we assume that \mathbb{T}_h is conformal: that is, \mathbb{T}_h is a simplicial mesh of $\overline{\Omega}$ without hanging nodes.

Let \mathcal{F}_h^i be the set of interior faces and \mathcal{F}_h^∂ the set of the faces on the boundary $\partial\Omega$. We set $\mathcal{F}_h := \mathcal{F}_h^i \cup \mathcal{F}_h^\partial$. For any $F \in \mathcal{F}_h$, we define the unit normal n_F to F as follows. (i) If $F \in \mathcal{F}_h^i$ with $F = T_1 \cap T_2$, $T_1, T_2 \in \mathbb{T}_h$, let n_1 and n_2 be the outward unit normals of T_1 and T_2 , respectively. Then, n_F is either of $\{n_1, n_2\}$; (ii) If $F \in \mathcal{F}_h^\partial$, n_F is the unit outward normal n to $\partial\Omega$.

Here, we consider \mathbb{R}^q -valued functions for some $q \in \mathbb{N}$. We define a broken (piecewise) Hilbert space as

$$H^1(\mathbb{T}_h)^q := \{v \in L^2(\Omega)^q : v|_T \in H^1(T)^q \quad \forall T \in \mathbb{T}_h\}$$

with the norms

$$\|v\|_{H^1(\mathbb{T}_h)^q} := \left(\sum_{T \in \mathbb{T}_h} \|v\|_{H^1(T)^q}^2 \right)^{\frac{1}{2}}.$$

When $q = 1$, we denote $H^1(\mathbb{T}_h) := H^1(\mathbb{T}_h)^1$. Let $\varphi \in H^1(\mathbb{T}_h)$. Suppose that $F \in \mathcal{F}_h^i$ with $F = T_1 \cap T_2$, $T_1, T_2 \in \mathbb{T}_h$. Set $\varphi_1 := \varphi|_{T_1}$ and $\varphi_2 := \varphi|_{T_2}$. Set two nonnegative real numbers $\omega_{T_1,F}$ and $\omega_{T_2,F}$ such that

$$\omega_{T_1,F} + \omega_{T_2,F} = 1.$$

The jump and the skew-weighted average of φ across F is then defined as

$$\llbracket \varphi \rrbracket := \llbracket \varphi \rrbracket_F := \varphi_1 - \varphi_2, \quad \{\{\varphi\}\}_{\bar{\omega}} := \{\{\varphi\}\}_{\bar{\omega},F} := \omega_{T_2,F}\varphi_1 + \omega_{T_1,F}\varphi_2.$$

For a boundary face $F \in \mathcal{F}_h^\partial$ with $F = \partial T \cap \partial\Omega$, $\llbracket \varphi \rrbracket_F := \varphi|_T$ and $\{\{\varphi\}\}_{\bar{\omega}} := \varphi|_T$. For any $v \in H^1(\mathbb{T}_h)^d$, we use the notation

$$\begin{aligned} \llbracket v \cdot n \rrbracket &:= \llbracket v \cdot n \rrbracket_F := v_1 \cdot n_F - v_2 \cdot n_F, \quad \{\{v\}\}_\omega := \{\{v\}\}_{\omega,F} := \omega_{T_1,F}v_1 + \omega_{T_2,F}v_2, \\ \llbracket v \rrbracket &:= \llbracket v \rrbracket_F := v_1 - v_2, \end{aligned}$$

for the jump of the normal component of v , the weighted average of v , and the jump of v .

We define a broken gradient operator as follows. For $\varphi \in H^1(\mathbb{T}_h)^d$, the broken gradient $\nabla_h : H^1(\mathbb{T}_h)^d \rightarrow L^2(\Omega)^{d \times d}$ is defined by

$$(\nabla_h \varphi)|_T := \nabla(\varphi|_T) \quad \forall T \in \mathbb{T}_h.$$

For all $T \in \mathbb{T}_h$, we define the broken $H(\text{div}; T)$ space as

$$H(\text{div}; \mathbb{T}_h) := \{v \in L^2(\Omega)^d; v|_T \in H(\text{div}; T) \quad \forall T \in \mathbb{T}_h\},$$

and the broken divergence operator $\text{div}_h : H(\text{div}; \mathbb{T}_h) \rightarrow L^2(\Omega)$ such that for all $v \in H(\text{div}; \mathbb{T}_h)$,

$$(\text{div}_h v)|_T := \text{div}(v|_T) \quad \forall T \in \mathbb{T}_h.$$

Let $T \in \mathbb{T}_h$. For any $k \in \mathbb{N}_0$, let $\mathbb{P}^k(T)$ be the space of polynomials with degree at most k in T . For any $F \in \mathcal{F}_h$, we define the L^2 -projection $\Pi_F^0 : L^2(F) \rightarrow \mathbb{P}^0(F)$ by

$$\int_F (\Pi_F^0 \varphi - \varphi) ds = 0 \quad \forall \varphi \in L^2(F).$$

2.4 Penalty parameters and energy norms

Deriving an appropriate penalty term is essential in discontinuous Galerkin methods (dG) on anisotropic meshes. The use of weighted averages gives robust dG schemes for various problems; see [20, 45]. For any $v \in H^1(\mathbb{T}_h)^d$ and $\varphi \in H^1(\mathbb{T}_h)$,

$$\llbracket (v\varphi) \cdot n \rrbracket_F = \{\{v\}\}_{\omega,F} \cdot n_F \llbracket \varphi \rrbracket_F + \llbracket v \cdot n \rrbracket_F \{\{\varphi\}\}_{\bar{\omega},F}.$$

For example, if $u \in H_0^1(\Omega) \cap W^{2,1}(\Omega)$, setting $v := -\nabla u$, we have $\llbracket v \cdot n \rrbracket_F = 0$ for all $F \in \mathcal{F}_h^i$, see [45, Lemma 4.3]. Using the trace (Lemma 1) and the

Hölder inequalities, the weighted average gives the following estimate for the term $\{\{v\}\}_{\omega,F} \cdot n_F \llbracket \varphi \rrbracket_F$.

$$\begin{aligned}
& \int_F |\{\{v\}\}_{\omega,F} \cdot n_F \llbracket \varphi \rrbracket_F| ds \\
& \leq c \left(\omega_{T_1,F} \|v|_{T_1}\|_{H^1(T_1)^d} \sqrt{\ell_{T_1,F}^{-1}} + \omega_{T_2,F} \|v|_{T_2}\|_{H^1(T_2)^d} \sqrt{\ell_{T_2,F}^{-1}} \right) \|\llbracket \varphi \rrbracket\|_{L^2(F)} \\
& \leq c \left(\|v|_{T_1}\|_{H^1(T_1)^d}^2 + \|v|_{T_2}\|_{H^1(T_2)^d}^2 \right)^{\frac{1}{2}} \left(\omega_{T_1,F}^2 \ell_{T_1,F}^{-1} + \omega_{T_2,F}^2 \ell_{T_2,F}^{-1} \right)^{\frac{1}{2}} \|\llbracket \varphi \rrbracket\|_{L^2(F)} \\
& = ch^\beta \left(\|v|_{T_1}\|_{H^1(T_1)^d}^2 + \|v|_{T_2}\|_{H^1(T_2)^d}^2 \right)^{\frac{1}{2}} \\
& \quad \times \left(h^{-2\beta} \omega_{T_1,F}^2 \ell_{T_1,F}^{-1} + h^{-2\beta} \omega_{T_2,F}^2 \ell_{T_2,F}^{-1} \right)^{\frac{1}{2}} \|\llbracket \varphi \rrbracket\|_{L^2(F)}, \tag{2.9}
\end{aligned}$$

where $\ell_{T_1,F}$ and $\ell_{T_2,F}$ are defined in the inequality (2.8). The weights $\omega_{T_1,F}$, $\omega_{T_2,F}$ and β are nonnegative real numbers chosen latter on. The associated penalty parameter when $\omega_{T_1,F} = \omega_{T_2,F} = \frac{1}{2}$ becomes

$$\frac{1}{4} h^{-2\beta} \left(\frac{1}{\ell_{T_1,F}} + \frac{1}{\ell_{T_2,F}} \right), \tag{2.10}$$

also see [39]. Furthermore,

$$\begin{aligned}
\frac{1}{4} h^{-2\beta} \max \left\{ \frac{1}{\ell_{T_1,F}}, \frac{1}{\ell_{T_2,F}} \right\} & \leq \frac{1}{4} h^{-2\beta} \left(\frac{1}{\ell_{T_1,F}} + \frac{1}{\ell_{T_2,F}} \right) \\
& \leq \frac{1}{2} h^{-2\beta} \max \left\{ \frac{1}{\ell_{T_1,F}}, \frac{1}{\ell_{T_2,F}} \right\}.
\end{aligned}$$

Another choice for the weighted parameters is such that for $F \in \mathcal{F}_h^i$ with $F = T_1 \cap T_2$, $T_1, T_2 \in \mathbb{T}_h$,

$$\omega_{T_i,F} := \frac{\sqrt{\ell_{T_i,F}}}{\sqrt{\ell_{T_1,F}} + \sqrt{\ell_{T_2,F}}}, \quad i = 1, 2. \tag{2.11}$$

Then, the associated penalty parameter is defined as

$$\frac{2h^{-2\beta}}{(\sqrt{\ell_{T_1,F}} + \sqrt{\ell_{T_2,F}})^2}. \tag{2.12}$$

This quantity is the special case of the parameter proposed in [20]. Given that

$$\begin{aligned}
\frac{2h^{-2\beta}}{(\sqrt{\ell_{T_1,F}} + \sqrt{\ell_{T_2,F}})^2} & \leq \frac{2h^{-2\beta}}{(2 \min\{\sqrt{\ell_{T_1,F}}, \sqrt{\ell_{T_2,F}}\})^2} = \frac{h^{-2\beta}}{2 \min\{\ell_{T_1,F}, \ell_{T_2,F}\}} \\
& \leq \frac{1}{2} h^{-2\beta} \left(\frac{1}{\ell_{T_1,F}} + \frac{1}{\ell_{T_2,F}} \right),
\end{aligned}$$

the quantity (2.12) makes (2.9) a shaper bound on anisotropic meshes than the parameter (2.10) for sufficiently small h . See also Remark 2.

Therefore, we use the type (2.12) of the parameter. For any $F \in \mathcal{F}_h$, we set $h_F := \text{diam}(F)$. Let $F \in \mathcal{F}_h^i$ with $F = T_1 \cap T_2$, $T_1, T_2 \in \mathbb{T}_h$ be an interior face and $F \in \mathcal{F}_h^\partial$ with $F = \partial T_\partial \cap \partial \Omega$, $T_\partial \in \mathbb{T}_h$ a boundary face. A new penalty parameter κ_F for the WOPSIP method is defined as follows using (2.12) with $\beta = 1$.

$$\kappa_F := \begin{cases} h^{-2} \left(\sqrt{\ell_{T_1, F}} + \sqrt{\ell_{T_2, F}} \right)^{-2} & \text{if } F \in \mathcal{F}_h^i, \\ h^{-2} \ell_{T_\partial, F}^{-1} & \text{if } F \in \mathcal{F}_h^\partial. \end{cases} \quad (2.13)$$

For the proof of the discrete Poincaré inequality (Lemma 6), we use the following parameter.

$$\kappa_{F^*} := \begin{cases} \left(\sqrt{\ell_{T_1, F}} + \sqrt{\ell_{T_2, F}} \right)^{-2} & \text{if } F \in \mathcal{F}_h^i, \\ \ell_{T_\partial, F}^{-1} & \text{if } F \in \mathcal{F}_h^\partial. \end{cases} \quad (2.14)$$

Remark 2 We set $s := \left(\frac{1}{2}\right)^\varepsilon$ for $\varepsilon \in \mathbb{R}$ and $\varepsilon > 1$. Let T_1 be the triangle with vertices $(0, 0)^T$, $(s, 0)^T$, and $(s, 1)^T$, and let T_2 be the triangle with vertices $(s, 0)^T$, $(1, 0)^T$, and $(s, 1)^T$. Then, we have $F = \{s\} \times (0, 1)$, $\ell_{T_1, F} = s$, $\ell_{T_2, F} = 1 - s$, $h = \sqrt{(1-s)^2 + 1}$, and

$$\begin{aligned} \kappa_F &= h^{-2} \left(\sqrt{\ell_{T_1, F}} + \sqrt{\ell_{T_2, F}} \right)^{-2} \rightarrow \frac{1}{2} \quad \text{as } \varepsilon \rightarrow \infty, \\ \kappa_{F^*} &= \left(\sqrt{\ell_{T_1, F}} + \sqrt{\ell_{T_2, F}} \right)^{-2} \rightarrow 1 \quad \text{as } \varepsilon \rightarrow \infty. \end{aligned}$$

However, the quantity given in (2.10) with $\beta = 0$ diverges as follows.

$$\frac{1}{4} \left(\frac{1}{\ell_{T_1, F}} + \frac{1}{\ell_{T_2, F}} \right) \rightarrow \infty \quad \text{as } \varepsilon \rightarrow \infty.$$

Remark 3 We set $s := \left(\frac{1}{2}\right)^\varepsilon$ for $\varepsilon \in \mathbb{R}$ and $\varepsilon > 1$. Let T_3 be the triangle with vertices $(0, 0)^T$, $(s, 0)^T$, and $(s, 1)^T$. Let T_4 be the triangle with vertices $(s, 0)^T$, $(2s, 0)^T$, and $(s, 1)^T$. Then, we have $F = \{s\} \times (0, 1)$, $\ell_{T_3, F} = s$, $\ell_{T_4, F} = s$, $h = \sqrt{s^2 + 1}$, and

$$\begin{aligned} \kappa_F &= h^{-2} \left(\sqrt{\ell_{T_3, F}} + \sqrt{\ell_{T_4, F}} \right)^{-2} \rightarrow \infty \quad \text{as } \varepsilon \rightarrow \infty, \\ \kappa_{F^*} &= \left(\sqrt{\ell_{T_1, F}} + \sqrt{\ell_{T_2, F}} \right)^{-2} \rightarrow \infty \quad \text{as } \varepsilon \rightarrow \infty. \end{aligned}$$

This may not be avoided by triangulation. Therefore, the use of anisotropic meshes may cause an ill-conditioned linear system.

Remark 4 To overcome this difficulty of Remark 3, we consider the following case. We set $s := \left(\frac{1}{2}\right)^\varepsilon$ for $\varepsilon \in \mathbb{R}$ and $\varepsilon > 1$. Let T_5 be the rectangle with vertices $(0, 0)^T$, $(s, 0)^T$, $(s, 1)^T$, and $(0, 1)^T$. Let T_6 be the triangle with vertices $(s, 0)^T$, $(1, 0)^T$, and $(s, 1)^T$. As in Remark 2, we have $F = \{s\} \times (0, 1)$, $\ell_{T_5, F} = s$, $\ell_{T_6, F} = 1 - s$, and $\kappa_F, \kappa_{F^*} \rightarrow 1$ as $\varepsilon \rightarrow \infty$. Therefore, the parameters may not be as large if quadrangles are used for elements adjacent to boundaries.

We define the following norms for any $v \in H^1(\mathbb{T}_h)$.

$$|v|_h := \left(|v|_{H^1(\mathbb{T}_h)}^2 + |v|_J^2 \right)^{\frac{1}{2}}$$

with the jump seminorm

$$|v|_J := \left(\sum_{F \in \mathcal{F}_h} \kappa_F \| \Pi_F^0 \llbracket v \rrbracket \|_{L^2(F)}^2 \right)^{\frac{1}{2}}$$

and κ_F defined as in (2.13);

$$|v|_{h_*} := \left(|v|_{H^1(\mathbb{T}_h)}^2 + |v|_{J_*}^2 \right)^{\frac{1}{2}}$$

with

$$|v|_{J_*} := \left(\sum_{F \in \mathcal{F}_h} \kappa_{F_*} \| \Pi_F^0 \llbracket v \rrbracket \|_{L^2(F)}^2 \right)^{\frac{1}{2}}$$

and κ_{F_*} defined as in (2.14). For any $v \in H^1(\mathbb{T}_h)$, $|v|_{J_*} \leq |v|_J$ for $h \leq 1$. The norm $|\cdot|_{h_*}$ is used to prove the discrete Poincaré inequality (Lemma 6).

2.5 Edge characterisation on a simplex, a geometric parameter, and a condition

Condition 1 (Case in which $d = 2$) Let $T \in \mathbb{T}_h$ with the vertices p_i ($i = 1, \dots, 3$). We assume that $\overline{p_2 p_3}$ is the longest edge of T ; i.e., $h_T := |p_2 - p_3|$. We set $h_1 = |p_1 - p_2|$ and $h_2 = |p_1 - p_3|$. We then assume that $h_2 \leq h_1$. Note that $h_1 \approx h_T$.

Condition 2 (Case in which $d = 3$) Let $T \in \mathbb{T}_h$ with the vertices p_i ($i = 1, \dots, 4$). Let L_i ($1 \leq i \leq 6$) be the edges of T . We denote by L_{\min} the edge of T with the minimum length; i.e., $|L_{\min}| = \min_{1 \leq i \leq 6} |L_i|$. We set $h_2 := |L_{\min}|$ and assume that

$$\text{the endpoints of } L_{\min} \text{ are either } \{p_1, p_3\} \text{ or } \{p_2, p_3\}.$$

Among the four edges that share an endpoint with L_{\min} , we take the longest edge $L_{\max}^{(\min)}$. Let p_1 and p_2 be the endpoints of edge $L_{\max}^{(\min)}$. We thus have that

$$h_1 = |L_{\max}^{(\min)}| = |p_1 - p_2|.$$

We consider cutting \mathbb{R}^3 with the plane that contains the midpoint of edge $L_{\max}^{(\min)}$ and is perpendicular to the vector $p_1 - p_2$. Thus, we have two cases:

- (Type i) p_3 and p_4 belong to the same half-space;
- (Type ii) p_3 and p_4 belong to different half-spaces.

In each case, we set

(Type i) p_1 and p_3 as the endpoints of L_{\min} , that is, $h_2 = |p_1 - p_3|$;
 (Type ii) p_2 and p_3 as the endpoints of L_{\min} , that is, $h_2 = |p_2 - p_3|$.

Finally, we set $h_3 = |p_1 - p_4|$. Note that we implicitly assume that p_1 and p_4 belong to the same half-space. In addition, note that $h_1 \approx h_T$.

We define vectors $r_n \in \mathbb{R}^d$, $n = 1, \dots, d$ as follows. If $d = 2$,

$$r_1 := \frac{p_2 - p_1}{|p_2 - p_1|}, \quad r_2 := \frac{p_3 - p_1}{|p_3 - p_1|},$$

and if $d = 3$,

$$r_1 := \frac{p_2 - p_1}{|p_2 - p_1|}, \quad r_3 := \frac{p_4 - p_1}{|p_4 - p_1|}, \quad \begin{cases} r_2 := \frac{p_3 - p_1}{|p_3 - p_1|}, & \text{for case (i),} \\ r_2 := \frac{p_3 - p_2}{|p_3 - p_2|} & \text{for case (ii).} \end{cases}$$

For a sufficiently smooth function φ and vector function $v := (v_1, \dots, v_d)^T$, we define the directional derivative as, for $i \in \{1 : d\}$,

$$\begin{aligned} \frac{\partial \varphi}{\partial r_i} &:= (r_i \cdot \nabla_x) \varphi = \sum_{i_0=1}^d (r_i)_{i_0} \frac{\partial \varphi}{\partial x_{i_0}}, \\ \frac{\partial v}{\partial r_i} &:= \left(\frac{\partial v_1}{\partial r_i}, \dots, \frac{\partial v_d}{\partial r_i} \right)^T = ((r_i \cdot \nabla_x) v_1, \dots, (r_i \cdot \nabla_x) v_d)^T. \end{aligned}$$

For a multi-index $\beta = (\beta_1, \dots, \beta_d) \in \mathbb{N}_0^d$, we use the notation

$$\partial_r^\beta \varphi := \frac{\partial^{|\beta|} \varphi}{\partial r_1^{\beta_1} \dots \partial r_d^{\beta_d}}, \quad h^\beta := h_1^{\beta_1} \dots h_d^{\beta_d}.$$

We proposed a geometric parameter H_T in a prior work [34].

Definition 1 The parameter H_T is defined as

$$H_T := \frac{\prod_{i=1}^d h_i}{|T|_d} h_T.$$

We introduce the geometric condition proposed in [34], which is equivalent to the maximum-angle condition [36].

Assumption 1 A family of meshes $\{\mathbb{T}_h\}$ has a semi-regular property if there exists $\gamma_0 > 0$ such that

$$\frac{H_T}{h_T} \leq \gamma_0 \quad \forall \mathbb{T}_h \in \{\mathbb{T}_h\}, \quad \forall T \in \mathbb{T}_h. \quad (2.15)$$

2.6 Affine mappings and Piola transformations

In anisotropic interpolation errors on anisotropic meshes, we follow a strategy proposed in several prior works [33,34,37]. Let $T \in \mathbb{T}_h$ with Condition 1 when $d = 2$ or Condition 2 when $d = 3$. We define an affine mapping $\Phi : \widehat{T} \rightarrow T$ as

$$\Phi : \widehat{T} \ni \hat{x} \mapsto x := \Phi(\hat{x}) := A_T \hat{x} + b_T \in T,$$

where $A_T \in \mathbb{R}^{d \times d}$ is an invertible matrix and $b_T \in \mathbb{R}^d$. See [37, Section 2].

The Piola transformation $\Psi : L^1(\widehat{T})^d \rightarrow L^1(T)^d$ is defined as

$$\begin{aligned} \Psi : L^1(\widehat{T})^d &\rightarrow L^1(T)^d \\ \hat{v} \mapsto v(x) &:= \Psi(\hat{v})(x) = \frac{1}{\det(A_T)} A_T \hat{v}(\hat{x}). \end{aligned}$$

2.7 Finite element spaces and anisotropic interpolation error estimates

For $k \in \mathbb{N}_0$, $\mathbb{P}^k(T)$ is spanned by the restriction to T of polynomials in \mathbb{P}^k where \mathbb{P}^k denotes the space of polynomials with degree at most k . Let Ne be the number of elements included in the mesh \mathbb{T}_h . Thus, we write $\mathbb{T}_h = \{T_j\}_{j=1}^{Ne}$.

2.7.1 Discontinuous space and the L^2 -orthogonal projection

For $T_j \in \mathbb{T}_h$, $j \in \{1, \dots, Ne\}$, let $\Pi_{T_j}^0 : L^2(T_j) \rightarrow \mathbb{P}^0$ be the L^2 -orthogonal projection defined as

$$\Pi_{T_j}^0 \varphi := \frac{1}{|T_j|_d} \int_{T_j} \varphi dx \quad \forall \varphi \in L^2(T_j).$$

The following theorem gives an anisotropic error estimate of the projection $\Pi_{T_j}^0$. Obtaining this estimate is not a novel concept [2]. However, the settings for meshes used in previous works differ slightly from our settings in Section 2.5. In our theory, the same estimate is obtained.

Theorem 2 For any $\hat{\varphi} \in H^1(\widehat{T})$ with $\varphi := \hat{\varphi} \circ \Phi^{-1}$,

$$\|\Pi_{T_j}^0 \varphi - \varphi\|_{L^2(T_j)} \leq c \sum_{i=1}^d h_i \left\| \frac{\partial \varphi}{\partial r_i} \right\|_{L^2(T_j)}. \quad (2.16)$$

Proof The scaling argument yields

$$\|\Pi_{T_j}^0 \varphi - \varphi\|_{L^2(T_j)} \leq c |\det(A_{T_j})|^{\frac{1}{2}} \|\Pi_{\widehat{T}}^0 \hat{\varphi} - \hat{\varphi}\|_{L^2(\widehat{T})}. \quad (2.17)$$

For any $\hat{\eta} \in \mathbb{P}^0$,

$$\|\Pi_{\widehat{T}}^0 \hat{\varphi} - \hat{\varphi}\|_{L^2(\widehat{T})} \leq \|\Pi_{\widehat{T}}^0(\hat{\varphi} - \hat{\eta})\|_{L^2(\widehat{T})} + \|\hat{\eta} - \hat{\varphi}\|_{L^2(\widehat{T})},$$

because $\Pi_{\hat{T}}^0 \hat{\eta} = \hat{\eta}$. The stability of the L^2 -orthogonal projection yields

$$\|\Pi_{\hat{T}}^0(\hat{\varphi} - \hat{\eta})\|_{L^2(\hat{T})} \leq c \|\hat{\varphi} - \hat{\eta}\|_{L^2(\hat{T})}.$$

Thus,

$$\|\Pi_{\hat{T}}^0 \hat{\varphi} - \hat{\varphi}\|_{L^2(\hat{T})} \leq c \inf_{\hat{\eta} \in \mathbb{P}^0} \|\hat{\varphi} - \hat{\eta}\|_{L^2(\hat{T})}. \quad (2.18)$$

From the Bramble–Hilbert-type lemma (e.g., see [17, Lemma 4.3.8]), there exists a constant $\hat{\eta}_\beta \in \mathbb{P}^0$ such that for any $\hat{\varphi} \in H^1(\hat{T})$,

$$\|\hat{\varphi} - \hat{\eta}_\beta\|_{L^2(\hat{T})} \leq C^{BH}(\hat{T}) |\hat{\varphi}|_{H^1(\hat{T})}. \quad (2.19)$$

Using the inequality in [37, Lemma 6] with $m = 0$ and $p = 2$, the inequality (2.19) is estimated as

$$\|\hat{\varphi} - \hat{\eta}_\beta\|_{L^2(\hat{T})} \leq c |\hat{\varphi}|_{H^1(\hat{T})} \leq c |\det(A_{T_j})|^{-\frac{1}{2}} \sum_{i=1}^d h_i \left\| \frac{\partial \varphi}{\partial r_i} \right\|_{L^2(T_j)}. \quad (2.20)$$

From (2.17), (2.18), and (2.20), we have the target inequality (2.16). \square

2.7.2 Discontinuous CR finite element space, an associated interpolation operator, and a Stokes element

We introduce a discontinuous CR finite element space and an associated interpolation operator, as well as a Stokes element.

Let the points $\{P_{T_j,1}, \dots, P_{T_j,d+1}\}$ be the vertices of the simplex $T_j \in \mathbb{T}_h$ for $j \in \{1, \dots, Ne\}$. Let $F_{T_j,i}$ be the face of T_j opposite $P_{T_j,i}$ for $i \in \{1, \dots, d+1\}$. We set $P := \mathbb{P}^1$, and take a set $\Sigma_{T_j} := \{\chi_{T_j,i}^{CR}\}_{1 \leq i \leq d+1}$ of linear forms with its components such that for any $p \in \mathbb{P}^1$,

$$\chi_{T_j,i}^{CR}(p) := \frac{1}{|F_{T_j,i}|^{d-1}} \int_{F_{T_j,i}} p ds \quad \forall i \in \{1, \dots, d+1\}. \quad (2.21)$$

For each $j \in \{1, \dots, Ne\}$, the triple $\{T_j, \mathbb{P}^1, \Sigma_{T_j}\}$ is a finite element. Using the barycentric coordinates $\{\lambda_{T_j,i}\}_{i=1}^{d+1} : \mathbb{R}^d \rightarrow \mathbb{R}$ on the reference element, the nodal basis functions associated with the degrees of freedom by (2.21) are defined as

$$\theta_{T_j,i}^{CR}(x) := d \left(\frac{1}{d} - \lambda_{T_j,i}(x) \right) \quad \forall i \in \{1, \dots, d+1\}. \quad (2.22)$$

For $j \in \{1, \dots, Ne\}$ and $i \in \{1, \dots, d+1\}$, we define the function $\phi_{j(i)}$ as

$$\phi_{j(i)}(x) := \begin{cases} \theta_{T_j,i}^{CR}(x), & x \in T_j, \\ 0, & x \notin T_j. \end{cases} \quad (2.23)$$

We define a discontinuous finite element space as

$$X_{dc,h}^{CR} := \left\{ \sum_{j=1}^{Ne} \sum_{i=1}^{d+1} c_{j(i)} \phi_{j(i)}; c_{j(i)} \in \mathbb{R}, \forall i, j \right\} \subset P_{dc,h}^1. \quad (2.24)$$

For $s \in \mathbb{N}_0$, we define a discontinuous finite element space as

$$P_{dc,h}^s := \left\{ p_h \in L^2(\Omega); p_h|_{T_j} \circ \Phi \in \mathbb{P}^s(\widehat{T}) \quad \forall T_j \in \mathbb{T}_h, \quad j \in \{1, \dots, Ne\} \right\}.$$

We define a pair of the standard dG spaces $(V_h^{m_1}, Q_h^{m_2})$ as

$$V_{dc,h}^{m_1} := (P_{dc,h}^{m_1})^d, \quad Q_h^{m_2} := P_{dc,h}^{m_2} \cap Q,$$

for $m_1 \in \mathbb{N}$ and $m_2 \in \mathbb{N}_0$. We use the discrete space $(V_{dc,h}^{m_1}, Q_h^{m_2})$ in Section 4.1. Let $(V_{dc,h}^{CR}, Q_h^0)$ be a pair of discontinuous finite element spaces defined by

$$V_{dc,h}^{CR} := (X_{dc,h}^{CR})^d, \quad Q_h^0 = P_{dc,h}^0 \cap Q, \quad (2.25)$$

with norms

$$|v_h|_{V_{dc,h}^{CR}} := \left(\sum_{i=1}^d |v_{h,i}|_h^2 \right)^{\frac{1}{2}}, \quad \|q_h\|_{Q_h^0} := \|q_h\|_{L^2(\Omega)}$$

for any $v_h = (v_{h,1}, \dots, v_{h,d})^T \in V_{dc,h}^{CR}$ and $q_h \in Q_h^0$. We use the discrete space $(V_{dc,h}^{CR}, Q_h^0)$ in the WOPSIP method (Section 3).

Let $I_{T_j}^{CR} : H^1(T_j) \rightarrow \mathbb{P}^1(T_j)$ be the CR interpolation operator such that for any $\varphi \in H^1(T_j)$,

$$I_{T_j}^{CR} : H^1(T_j) \ni \varphi \mapsto I_{T_j}^{CR} \varphi := \sum_{i=1}^{d+1} \left(\frac{1}{|F_{T_j,i}|^{d-1}} \int_{F_{T_j,i}} \varphi ds \right) \theta_{T_j,i}^{CR} \in \mathbb{P}^1(T_j). \quad (2.26)$$

We then present estimates of the anisotropic CR interpolation error. Obtaining the estimate is not a novel concept [3]. However, the proof provided here differs from those given in prior works. We here present a proof using the error estimate of the L^2 -projection Π_h^0 in Theorem 2.

Theorem 3 For $j \in \{1, \dots, Ne\}$,

$$|I_{T_j}^{CR} \varphi - \varphi|_{H^1(T_j)} \leq c \sum_{i=1}^d h_i \left\| \frac{\partial}{\partial r_i} \nabla \varphi \right\|_{L^2(T_j)^d} \quad \forall \varphi \in H^2(T_j). \quad (2.27)$$

Proof Let $\varphi \in H^2(T_j)$, $j \in \{1, \dots, Ne\}$. Because $I_{T_j}^{CR}\varphi \in \mathbb{P}^1$, Green's formula and the definition of the CR interpolation imply that

$$\begin{aligned} \frac{\partial}{\partial x_k}(I_{T_j}^{CR}\varphi) &= \frac{1}{|T_j|^d} \int_{T_j} \frac{\partial}{\partial x_k}(I_{T_j}^{CR}\varphi) dx = \frac{1}{|T_j|^d} \sum_{i=1}^{d+1} n_{T_j}^{(k)} \int_{F_i} I_{T_j}^{CR}\varphi ds \\ &= \frac{1}{|T_j|^d} \sum_{i=1}^{d+1} n_{T_j}^{(k)} \int_{F_i} \varphi ds = \frac{1}{|T_j|^d} \int_{T_j} \frac{\partial \varphi}{\partial x_k} dx = \Pi_{T_j}^0 \left(\frac{\partial \varphi}{\partial x_k} \right), \end{aligned}$$

for $k \in \{1, \dots, d\}$, where $n_{T_j}^{(k)}$ denotes the k th component of the outer unit normal vector n_{T_j} . The inequality (2.16) yields

$$\begin{aligned} |I_{T_j}^{CR}\varphi - \varphi|_{H^1(T_j)}^2 &= \sum_{k=1}^d \left\| \frac{\partial}{\partial x_k}(I_{T_j}^{CR}\varphi - \varphi) \right\|_{L^2(T_j)}^2 \\ &= \sum_{k=1}^d \left\| \Pi_{T_j}^0 \left(\frac{\partial \varphi}{\partial x_k} \right) - \left(\frac{\partial \varphi}{\partial x_k} \right) \right\|_{L^2(T_j)}^2 \leq c \sum_{i,k=1}^d h_i^2 \left\| \frac{\partial^2 \varphi}{\partial r_i \partial x_k} \right\|_{L^2(T_j)}^2, \end{aligned}$$

which leads to (2.27) together with the Jensen's inequality. \square

The vector-valued local interpolation operator

$$\mathcal{I}_{T_j}^{CR} : H^1(T_j)^d \rightarrow \mathbb{P}^1(T_j)^d \quad (2.28)$$

is defined component-wise, that is,

$$\mathcal{I}_{T_j}^{CR} v := (I_{T_j}^{CR} v_1, \dots, I_{T_j}^{CR} v_d)^T \quad \forall v = (v_1, \dots, v_d)^T \in H^1(T_j)^d.$$

We define a global interpolation operator $\mathcal{I}_h^{CR} : H^1(\Omega)^d \rightarrow V_{dc,h}^{CR}$ as

$$(\mathcal{I}_h^{CR} v)|_{T_j} = \mathcal{I}_{T_j}^{CR}(v|_{T_j}), \quad j \in \{1, \dots, Ne\}, \quad \forall v \in H^1(\Omega)^d. \quad (2.29)$$

2.7.3 Discontinuous RT finite element space and an associated interpolation operator

We introduce a discontinuous RT finite element space and an associated interpolation operator.

For $T_j \in \mathbb{T}_h$, $j \in \{1, \dots, Ne\}$, we define the local RT polynomial space as follows.

$$\mathbb{RT}^0(T_j) := \mathbb{P}^0(T_j)^d + x\mathbb{P}^0(T_j), \quad x \in \mathbb{R}^d. \quad (2.30)$$

For $p \in \mathbb{RT}^0(T_j)$, the local degrees of freedom are defined as

$$\chi_{T_j,i}^{RT}(p) := \int_{F_{T_j,i}} p \cdot n_{T_j,i} ds \quad \forall i \in \{1, \dots, d+1\}, \quad (2.31)$$

where $n_{T_j,i}$ is the outward normal to $F_{T_j,i}$. Setting $\Sigma_{T_j}^{RT} := \{\chi_{T_j,i}^{RT}\}_{1 \leq i \leq d+1}$, the triple $\{T_j, \mathbb{RT}^0, \Sigma_{T_j}^{RT}\}$ a finite element. The local shape functions are

$$\theta_{T_j,i}^{RT}(x) := \frac{\iota_{F_{T_j,i},T_j}}{d|T_j|_d}(x - P_{T_j,i}) \quad \forall i \in \{1, \dots, d+1\}, \quad (2.32)$$

where $\iota_{F_{T_j,i},T_j} := 1$ if $n_{T_j,i}$ points outwards, and -1 otherwise [23]. We define a discontinuous RT finite element space as follows.

$$V_{dc,h}^{RT} := \{v_h \in L^1(\Omega)^d : v_h|_T \in \mathbb{RT}^0(T) \quad \forall T \in \mathbb{T}_h\}. \quad (2.33)$$

Let $\mathcal{I}_{T_j}^{RT} : H^1(T_j)^d \rightarrow \mathbb{RT}^0(T_j)$ be the RT interpolation operator such that for any $v \in H^1(T_j)^d$,

$$\mathcal{I}_{T_j}^{RT} : H^1(T_j)^d \ni v \mapsto \mathcal{I}_{T_j}^{RT} v := \sum_{i=1}^{d+1} \left(\int_{F_{T_j,i}} v \cdot n_{T_j,i} ds \right) \theta_{T_j,i}^{RT} \in \mathbb{RT}^0(T_j). \quad (2.34)$$

The following two theorems are divided into the element of (Type i) or the element of (Type ii) in Section 2.5 when $d = 3$.

Theorem 4 *Let T_j be the element with Conditions 1 or 2 and satisfy (Type i) in Section 2.5 when $d = 3$. For any $\hat{v} \in H^1(\hat{T})^d$ with $v = (v_1, \dots, v_d)^T := \Psi \hat{v}$ and $j \in \{1, \dots, Ne\}$,*

$$\|\mathcal{I}_{T_j}^{RT} v - v\|_{L^2(T_j)^d} \leq c \left(\frac{H_{T_j}}{h_{T_j}} \sum_{i=1}^d h_i \left\| \frac{\partial v}{\partial r_i} \right\|_{L^2(T_j)^d} + h_{T_j} \|\operatorname{div} v\|_{L^2(T_j)} \right). \quad (2.35)$$

Proof A proof is provided in [33, Theorem 2]. \square

Theorem 5 *Let $d = 3$. Let T_j be an element with Condition 2 that satisfies (Type ii) in Section 2.5. For $\hat{v} \in H^1(\hat{T})^3$ with $v = (v_1, v_2, v_3)^T := \Psi \hat{v}$ and $j \in \{1, \dots, Ne\}$,*

$$\|\mathcal{I}_{T_j}^{RT} v - v\|_{L^2(T_j)^3} \leq c \frac{H_{T_j}}{h_{T_j}} \left(h_{T_j} |v|_{H^1(T_j)^3} \right). \quad (2.36)$$

Proof A proof is provided in [33, Theorem 3]. \square

We define a global interpolation operator $\mathcal{I}_h^{RT} : H^1(\Omega)^d \cup V_{dc,h}^{CR} \rightarrow V_{dc,h}^{RT}$ by

$$(\mathcal{I}_h^{RT} v)|_{T_j} = \mathcal{I}_{T_j}^{RT}(v|_{T_j}), \quad j \in \{1, \dots, Ne\}, \quad \forall v \in H^1(\Omega)^d \cup V_{dc,h}^{CR}. \quad (2.37)$$

We also define the global interpolation Π_h^0 to the space $P_{dc,h}^0$ as

$$(\Pi_h^0 \varphi)|_{T_j} := \Pi_T^0(\varphi|_{T_j}) \quad \forall T_j \in \mathbb{T}_h, \quad j \in \{1, \dots, Ne\}, \quad \forall \varphi \in L^2(\Omega).$$

Between the RT interpolation \mathcal{I}_h^{RT} and the L^2 -projection Π_h^0 , the following relation holds.

Lemma 2 For $j \in \{1, \dots, Ne\}$,

$$\operatorname{div}(\mathcal{I}_{T_j}^{RT} v) = \Pi_{T_j}^0(\operatorname{div} v) \quad \forall v \in H^1(T_j)^d. \quad (2.38)$$

By combining (2.38), for any $v \in H^1(\Omega)^d$

$$\operatorname{div}(\mathcal{I}_h^{RT} v) = \Pi_h^0(\operatorname{div} v). \quad (2.39)$$

Proof A proof is provided in [23, Lemma 16.2]. \square

3 WOPSIP method for the Stokes equation

This section provides an analysis of the WOPSIP method for the Stokes equations on anisotropic meshes.

3.1 WOPSIP method

We consider the WOPSIP method for the Stokes equation (2.2) as follows. We aim to find $(u_h, p_h) \in V_{dc,h}^{CR} \times Q_h^0$ such that

$$\nu a_h^{wop}(u_h, v_h) + b_h(v_h, p_h) = \int_{\Omega} f \cdot v_h dx \quad \forall v_h \in V_{dc,h}^{CR}, \quad (3.1a)$$

$$b_h(u_h, q_h) = 0 \quad \forall q_h \in Q_h^0, \quad (3.1b)$$

where $a_h^{wop} : (V + V_{dc,h}^{CR}) \times (V + V_{dc,h}^{CR}) \rightarrow \mathbb{R}$ and $b_h : (V + V_{dc,h}^{CR}) \times Q_h^0 \rightarrow \mathbb{R}$ respectively denote bilinear forms defined by

$$a_h^{wop}(u_h, v_h) := \sum_{i=1}^d a_h^i(u_{h,i}, v_{h,i}),$$

$$a_h^i(u_{h,i}, v_{h,i}) := \int_{\Omega} \nabla_h u_{h,i} \cdot \nabla_h v_{h,i} dx + \sum_{F \in \mathcal{F}_h} \kappa_F \int_F \Pi_F^0[[u_{h,i}]] \Pi_F^0[[v_{h,i}]] ds,$$

$$b_h(v_h, q_h) := - \int_{\Omega} \operatorname{div}_h v_h q_h dx,$$

where $\{u_{h,i}\}_{i=1}^d$ and $\{v_{h,i}\}_{i=1}^d$ respectively denote the Cartesian components of u_h and v_h . Recall that the parameter κ_F is defined in (2.13). Using the Hölder's inequality, we obtain

$$|a_h^{wop}(u(h), v_h)| \leq c |u(h)|_{V_{dc,h}^{CR}} |v_h|_{V_{dc,h}^{CR}} \quad \forall u(h) \in V + V_{dc,h}^{CR}, \quad \forall v_h \in V_{dc,h}^{CR}, \quad (3.2)$$

$$|b_h(u(h), q_h)| \leq c |u(h)|_{V_{dc,h}^{CR}} \|q_h\|_{Q_h^0} \quad \forall u(h) \in V + V_{dc,h}^{CR}, \quad \forall q_h \in Q_h^0. \quad (3.3)$$

We set

$$V_{dc,h,\operatorname{div}}^{CR} := \{v_h \in V_{dc,h}^{CR}; b_h(v_h, q_h) = 0 \quad \forall q_h \in Q_h^0\}.$$

We then observe that

$$\nu a_h^{wop}(v_h, v_h) = \nu |v_h|_{V_{dc,h}^{CR}}^2 \quad \forall v_h \in V_{dc,h,\operatorname{div}}^{CR}.$$

Remark 5 Let x_F be the barycentre point of $F \in \mathcal{F}_h$. Let $F \in \mathcal{F}_h^i$ with $F = T_1 \cap T_2$, $T_1, T_2 \in \mathbb{T}_h$. We define a finite element space as

$$V_{h0}^{CR} := \left\{ v_h \in V_{dc,h}^{CR}; v_h|_{T_1 \cap F}(x_F) = v_h|_{T_2 \cap F}(x_F) \quad \forall F \in \mathcal{F}_h^i, \right. \\ \left. v_h|_F(x_F) = 0 \quad \forall F \in \mathcal{F}_h^\partial \right\} \subset V_{dc,h}^{CR},$$

with a norm

$$|v_h|_{V_{h0}^{CR}} := |v_h|_{H^1(\mathbb{T}_h)^d}.$$

We note that the space V_{h0}^{CR} is the classical CR finite element space on a conforming mesh.

For $v_h \in V_{h0}^{CR}$, by the midpoint rule, for $F \in \mathcal{F}_h^i$,

$$\Pi_F^0[v_h] = \frac{1}{|F|^{d-1}} \int_F [v_h] ds = [v_h](x_F) = v_h|_{T_1 \cap F}(x_F) - v_h|_{T_2 \cap F}(x_F) = 0. \quad (3.4)$$

By an analogous argument,

$$\Pi_F^0 v_h|_F = 0 \quad \forall F \in \mathcal{F}_h^\partial. \quad (3.5)$$

3.2 Stability of the WOPSIP method

The following relation plays an important role in the discontinuous Galerkin finite element analysis on anisotropic meshes.

Lemma 3 For any $w \in H^1(\Omega)^d$ and $\psi_h \in P_{dc,h}^1$,

$$\int_{\Omega} (\mathcal{I}_h^{RT} w \cdot \nabla_h \psi_h + \operatorname{div} \mathcal{I}_h^{RT} w \psi_h) dx \\ = \sum_{F \in \mathcal{F}_h^i} \int_F \{ \{w\} \}_{\omega, F} \cdot n_F \Pi_F^0 [\psi_h]_F ds + \sum_{F \in \mathcal{F}_h^\partial} \int_F (w \cdot n_F) \Pi_F^0 \psi_h ds. \quad (3.6)$$

Proof For any $w \in H^1(\Omega)^d$ and $\psi_h \in P_{dc,h}^1$, using Green's formula and the fact $\mathcal{I}_h^{RT} w \cdot n_F \in \mathbb{P}^0(F)$ for any $F \in \mathcal{F}_h$, we derive

$$\int_{\Omega} (\mathcal{I}_h^{RT} w \cdot \nabla_h \psi_h + \operatorname{div} \mathcal{I}_h^{RT} w \psi_h) dx = \sum_{T \in \mathbb{T}_h} \int_{\partial T} (\mathcal{I}_h^{RT} w \cdot n_T) \psi_h ds \\ = \sum_{F \in \mathcal{F}_h^i} \int_F ([\mathcal{I}_h^{RT} w \cdot n]_F \{ \{ \psi_h \} \}_{\bar{\omega}, F} + \{ \{ \mathcal{I}_h^{RT} w \} \}_{\omega, F} \cdot n_F [\psi_h]_F) ds \\ + \sum_{F \in \mathcal{F}_h^\partial} \int_F (\mathcal{I}_h^{RT} w \cdot n_F) \psi_h ds.$$

Recall that the weighted and skew-weighted averages $\{\{\cdot\}\}_{\omega,F}$ and $\{\{\cdot\}\}_{\bar{\omega},F}$ were defined in Section 2.3.

By the midpoint rule, we have

$$\begin{aligned} \llbracket \mathcal{I}_h^{RT} w \cdot n \rrbracket_F(x_F) &= \frac{1}{|F|^{d-1}} \int_F \llbracket \mathcal{I}_h^{RT} w \cdot n \rrbracket_F(x) ds \\ &= \frac{1}{|F|^{d-1}} \int_F \llbracket w \cdot n \rrbracket_F(x) ds = 0, \end{aligned}$$

which leads to

$$\llbracket \mathcal{I}_h^{RT} w \cdot n \rrbracket_F(x) = 0 \quad \forall x \in F. \quad (3.7)$$

Using (3.7) and the properties of the projection Π_F^0 and \mathcal{I}_h^{RT} yields

$$\begin{aligned} &\int_{\Omega} (\mathcal{I}_h^{RT} w \cdot \nabla_h \psi_h + \operatorname{div} \mathcal{I}_h^{RT} w \psi_h) dx \\ &= \sum_{F \in \mathcal{F}_h^i} \int_F \{\{\mathcal{I}_h^{RT} w\}\}_{\omega,F} \cdot n_F \Pi_F^0 \llbracket \psi_h \rrbracket_F ds + \sum_{F \in \mathcal{F}_h^\partial} \int_F (\mathcal{I}_h^{RT} w \cdot n_F) \Pi_F^0 \psi_h ds \\ &= \sum_{F \in \mathcal{F}_h^i} \int_F \{\{w\}\}_{\omega,F} \cdot n_F \Pi_F^0 \llbracket \psi_h \rrbracket_F ds + \sum_{F \in \mathcal{F}_h^\partial} \int_F (w \cdot n_F) \Pi_F^0 \psi_h ds, \end{aligned}$$

which is the desired equality. \square

The right-hand terms in (3.6) are estimated as follows.

Lemma 4 *For any $w \in H^1(\Omega)^d$ and $\psi_h \in P_{dc,h}^1$,*

$$\begin{aligned} &\left| \sum_{F \in \mathcal{F}_h^i} \int_F \{\{w\}\}_{\omega,F} \cdot n_F \Pi_F^0 \llbracket \psi_h \rrbracket_F ds \right| \\ &\leq c |\psi_h|_J \left(h \|w\|_{L^2(\Omega)^d} + h^{\frac{3}{2}} \|w\|_{L^2(\Omega)^d}^{\frac{1}{2}} |w|_{H^1(\Omega)^d}^{\frac{1}{2}} \right), \quad (3.8) \end{aligned}$$

$$\begin{aligned} &\left| \sum_{F \in \mathcal{F}_h^\partial} \int_F (w \cdot n_F) \Pi_F^0 \psi_h ds \right| \\ &\leq c |\psi_h|_J \left(h \|w\|_{L^2(\Omega)^d} + h^{\frac{3}{2}} \|w\|_{L^2(\Omega)^d}^{\frac{1}{2}} |w|_{H^1(\Omega)^d}^{\frac{1}{2}} \right), \quad (3.9) \end{aligned}$$

where \mathbb{T}_F denotes the set of the simplices in \mathbb{T}_h that share F as a common face.

Proof Using the Hölder's inequality, the weighted average and the trace inequality (2.8) yields

$$\begin{aligned} & \int_F | \{w\}_{\omega, F} \cdot n_F \Pi_F^0 [\psi_h]_F | ds \\ & \leq c \left\{ \left(\|w_1\|_{L^2(T_1)^d} + h_{T_1}^{\frac{1}{2}} \|w_1\|_{L^2(T_1)^d}^{\frac{1}{2}} |w_1|_{H^1(T_1)^d}^{\frac{1}{2}} \right)^2 \right. \\ & \quad \left. + \left(\|w_2\|_{L^2(T_2)^d} + h_{T_2}^{\frac{1}{2}} \|w_2\|_{L^2(T_2)^d}^{\frac{1}{2}} |w_2|_{H^1(T_2)^d}^{\frac{1}{2}} \right)^2 \right\}^{\frac{1}{2}} \\ & \quad \times \left(\omega_{T_1, F}^2 \ell_{T_1, F}^{-1} + \omega_{T_2, F}^2 \ell_{T_2, F}^{-1} \right)^{\frac{1}{2}} \|\Pi_F^0 [\psi_h]\|_{L^2(F)}. \end{aligned}$$

Using the Cauchy–Schwarz inequality,

$$\begin{aligned} & \left| \sum_{F \in \mathcal{F}_h^i} \int_F \{w\}_{\omega, F} \cdot n_F \Pi_F^0 [\psi_h]_F ds \right| \\ & \leq c \sum_{F \in \mathcal{F}_h^i} h^{-1} \left(\omega_{T_1, F}^2 \ell_{T_1, F}^{-1} + \omega_{T_2, F}^2 \ell_{T_2, F}^{-1} \right)^{\frac{1}{2}} \|\Pi_F^0 [\psi_h]\|_{L^2(F)} \\ & \quad \times \sum_{T \in \mathbb{T}_F} h \left(\|w\|_{L^2(T)^d} + h_T^{\frac{1}{2}} \|w\|_{L^2(T)^d}^{\frac{1}{2}} |w|_{H^1(T)^d}^{\frac{1}{2}} \right) \\ & \leq c \left(\sum_{F \in \mathcal{F}_h^i} h^{-2} \left(\omega_{T_1, F}^2 \ell_{T_1, F}^{-1} + \omega_{T_2, F}^2 \ell_{T_2, F}^{-1} \right) \|\Pi_F^0 [\psi_h]\|_{L^2(F)}^2 \right)^{\frac{1}{2}} \\ & \quad \times \left(\sum_{F \in \mathcal{F}_h^i} \sum_{T \in \mathbb{T}_F} h^2 \left(\|w\|_{L^2(T)^d} + h_T^{\frac{1}{2}} \|w\|_{L^2(T)^d}^{\frac{1}{2}} |w|_{H^1(T)^d}^{\frac{1}{2}} \right)^2 \right)^{\frac{1}{2}} \end{aligned}$$

which leads to the inequality (3.8) together with the weight (2.11) and the Cauchy–Schwarz and Jensen inequalities.

By an analogous argument, the estimate (3.9) holds. \square

Lemma 5 *Let $h \leq 1$. Thus, for any $w \in H^1(\Omega)^d$ and $\psi_h \in P_{dc, h}^1$,*

$$\left| \sum_{F \in \mathcal{F}_h^i} \int_F \{w\}_{\omega, F} \cdot n_F \Pi_F^0 [\psi_h]_F ds \right| \leq c |\psi_h|_{J^*} \|w\|_{H^1(\Omega)^d}, \quad (3.10)$$

$$\left| \sum_{F \in \mathcal{F}_h^o} \int_F (w \cdot n_F) \Pi_F^0 \psi_h ds \right| \leq c |\psi_h|_{J^*} \|w\|_{H^1(\Omega)^d}. \quad (3.11)$$

Proof By analogous proof with Lemma 4, we can obtain the target inequalities. \square

The following lemma provides a discrete Poincaré inequality. For simplicity, we assume that Ω is convex.

Lemma 6 (Discrete Poincaré inequality) *Assume that Ω is convex. Let $\{\mathbb{T}_h\}$ be a family of meshes with the semi-regular property (Assumption 1) and $h \leq 1$. Then, there exists a positive constant C_{dc}^P independent of h but dependent on the maximum angle such that*

$$\|\psi_h\|_{L^2(\Omega)} \leq C_{dc}^P |\psi_h|_{h^*} \quad \forall \psi_h \in P_{dc,h}^1. \quad (3.12)$$

Proof Let $\psi_h \in P_{dc,h}^1$. We consider the following problem. Find $z \in H^2(\Omega) \cap H_0^1(\Omega)$ such that

$$-\Delta z = \psi_h \quad \text{in } \Omega, \quad z = 0 \quad \text{on } \partial\Omega.$$

We then have a priori estimates $|z|_{H^1(\Omega)} \leq C_P \|\psi_h\|_{L^2(\Omega)}$ and $|z|_{H^2(\Omega)} \leq \|\psi_h\|_{L^2(\Omega)}$, where C_P is the Poincaré constant.

We provide the following equality for analysis.

$$\begin{aligned} \int_{\Omega} (\operatorname{div} \mathcal{I}_h^{RT}(\nabla z)) \psi_h dx &= \sum_{T \in \mathbb{T}_h} \int_{\partial T} n_T \cdot \mathcal{I}_h^{RT}(\nabla z) \psi_h ds - \int_{\Omega} \mathcal{I}_h^{RT}(\nabla z) \cdot \nabla_h \psi_h dx \\ &= \int_{\Omega} (\nabla z - \mathcal{I}_h^{RT}(\nabla z)) \cdot \nabla_h \psi_h dx - \int_{\Omega} \nabla z \cdot \nabla_h \psi_h dx \\ &\quad + \sum_{T \in \mathbb{T}_h} \int_{\partial T} \mathcal{I}_h^{RT}(\nabla z) \cdot n_T \psi_h ds \\ &= \int_{\Omega} (\nabla z - \mathcal{I}_h^{RT}(\nabla z)) \cdot \nabla_h \psi_h dx - \int_{\Omega} \nabla z \cdot \nabla_h \psi_h dx \\ &\quad + \sum_{F \in \mathcal{F}_h^i} \int_F \{ \{ \nabla z \} \}_{\omega, F} \cdot n_F \Pi_F^0[\psi_h]_F ds \\ &\quad + \sum_{F \in \mathcal{F}_h^\partial} \int_F (\nabla z \cdot n_F) \Pi_F^0 \psi_h ds, \end{aligned}$$

where we apply the analogous argument with Lemma 3 for the last equality. This equality yields

$$\begin{aligned} \|\psi_h\|_{L^2(\Omega)}^2 &= \int_{\Omega} \psi_h^2 dx = \int_{\Omega} -\Delta z \psi_h dx = - \int_{\Omega} \operatorname{div}(\nabla z) \psi_h dx \\ &= \int_{\Omega} (\Pi_h^0 \operatorname{div}(\nabla z) - \operatorname{div}(\nabla z)) \psi_h dx - \int_{\Omega} (\Pi_h^0 \operatorname{div}(\nabla z)) \psi_h dx \\ &= \int_{\Omega} (\Pi_h^0 \operatorname{div}(\nabla z) - \operatorname{div}(\nabla z)) (\psi_h - \Pi_h^0 \psi_h) dx - \int_{\Omega} (\operatorname{div} \mathcal{I}_h^{RT}(\nabla z)) \psi_h dx \\ &= - \int_{\Omega} \operatorname{div}(\nabla z) (\psi_h - \Pi_h^0 \psi_h) dx \\ &\quad - \int_{\Omega} (\nabla z - \mathcal{I}_h^{RT}(\nabla z)) \cdot \nabla_h \psi_h dx + \int_{\Omega} \nabla z \cdot \nabla_h \psi_h dx \end{aligned}$$

$$- \sum_{F \in \mathcal{F}_h^i} \int_F \{ \{ \nabla z \} \}_{\omega, F} \cdot n_F \Pi_F^0 \llbracket \psi_h \rrbracket_F ds - \sum_{F \in \mathcal{F}_h^\partial} \int_F (\nabla z \cdot n_F) \Pi_F^0 \psi_h ds.$$

Using the Hölder's inequality, the error estimates (2.16), (2.35), (2.36) and Lemma 6, we have

$$\begin{aligned} \|\psi_h\|_{L^2(\Omega)}^2 &\leq \|\Delta z\|_{L^2(\Omega)} \|\psi_h - \Pi_h^0 \psi_h\|_{L^2(\Omega)} + \|\nabla z - \mathcal{I}_h^{RT}(\nabla z)\|_{L^2(\Omega)} |\psi_h|_{H^1(\mathbb{T}_h)} \\ &\quad + |z|_{H^1(\Omega)} |\psi_h|_{H^1(\mathbb{T}_h)} + c \|\nabla z\|_{H^1(\Omega)^d} |\psi_h|_{J_*} \\ &\leq c(h+1) \|\psi_h\|_{L^2(\Omega)} |\psi_h|_{h^*}, \end{aligned}$$

which leads to the target inequality if $h \leq 1$. \square

We show the discrete inf-sup condition using Fortin's criterion [26].

Lemma 7 (Inf-sup stability) *The nonconforming Stokes element of type $V_{dc,h}^{CR} \times Q_h^0$ satisfies the uniform inf-sup stability condition*

$$\inf_{q_h \in Q_h^0} \sup_{v_h \in V_{dc,h}^{CR}} \frac{b_h(v_h, q_h)}{|v_h|_{V_{dc,h}^{CR}} \|q_h\|_{Q_h^0}} \geq \beta_* := \beta. \quad (3.13)$$

Proof Let $v \in V$ and $q_h \in Q_h^0$. Using $\nabla q_h \equiv 0$ on T and the definition of \mathcal{I}_h^{CR} , we obtain

$$\begin{aligned} b_h(v, q_h) &= \sum_{T \in \mathbb{T}_h} \int_T \operatorname{div} v q_h dx = \sum_{T \in \mathbb{T}_h} \int_{\partial T} (v \cdot n_T) q_h ds \\ &= \sum_{T \in \mathbb{T}_h} \int_{\partial T} (\mathcal{I}_h^{CR} v \cdot n_T) q_h ds = \sum_{T \in \mathbb{T}_h} \int_T \operatorname{div} (\mathcal{I}_h^{CR} v) q_h dx \\ &= b_h(\mathcal{I}_h^{CR} v, q_h). \end{aligned} \quad (3.14)$$

Given that $\Delta(I_T^{CR} v_i) \equiv 0$ on $T \in \mathbb{T}_h$ and $n_T \cdot \nabla(I_T^{CR} v_i) \in \mathcal{P}^0$ on faces of T , and using the definition of \mathcal{I}_h^{CR} and the Hölder's inequality, we have

$$\begin{aligned} |\mathcal{I}_h^{CR} v|_{H^1(\mathbb{T}_h)^d}^2 &= \sum_{T \in \mathbb{T}_h} \sum_{i=1}^d |I_T^{CR} v_i|_{H^1(T)}^2 = \sum_{T \in \mathbb{T}_h} \sum_{i=1}^d \int_{\partial T} n_T \cdot \nabla(I_T^{CR} v_i) I_T^{CR} v_i ds \\ &= \sum_{T \in \mathbb{T}_h} \sum_{i=1}^d \int_T \nabla(I_T^{CR} v_i) \cdot \nabla v_i dx \leq |\mathcal{I}_h^{CR} v|_{H^1(\mathbb{T}_h)^d} |v|_{H^1(\Omega)^d}, \end{aligned}$$

which leads to

$$|\mathcal{I}_h^{CR} v|_{H^1(\mathbb{T}_h)^d} \leq |v|_{H^1(\Omega)^d}. \quad (3.15)$$

Using the definition of the L^2 -projection Π_F^0 and the definition of $\mathcal{I}_h^{CR} v$, we have for $i = 1, \dots, d$,

$$\begin{aligned} \|\Pi_F^0 \llbracket (\mathcal{I}_h^{CR} v)_i \rrbracket\|_{L^2(F)}^2 &= \int_F \Pi_F^0 \llbracket (\mathcal{I}_h^{CR} v)_i \rrbracket \Pi_F^0 \llbracket (\mathcal{I}_h^{CR} v)_i \rrbracket ds \\ &= \int_F \llbracket v_i \rrbracket \Pi_F^0 \llbracket (\mathcal{I}_h^{CR} v)_i \rrbracket ds = 0, \end{aligned} \quad (3.16)$$

because $[[v_i]]_F = 0$ for $v_i \in H_0^1(\Omega)$ and $i \in \{1, \dots, d\}$.

Let $q_h \in Q_h^0$. Using the continuous inf-sup condition (2.4), (3.14), (3.15) and (3.16), we have

$$\begin{aligned} \beta \|q_h\|_{Q_h^0} &\leq \sup_{v \in V} \frac{b(v, q_h)}{|v|_{H^1(\Omega)^d}} = \sup_{v \in V} \frac{b(\mathcal{I}_h^{CR} v, q_h)}{|\mathcal{I}_h^{CR} v|_{V_{dc,h}^{CR}}} \frac{|\mathcal{I}_h^{CR} v|_{V_{dc,h}^{CR}}}{|v|_{H^1(\Omega)^d}} \\ &\leq \sup_{v \in V} \frac{b(\mathcal{I}_h^{CR} v, q_h)}{|\mathcal{I}_h^{CR} v|_{V_{dc,h}^{CR}}} \leq \sup_{v_h \in V_{dc,h}^{CR}} \frac{b(v_h, q_h)}{|v_h|_{V_{dc,h}^1}}, \end{aligned}$$

which is the target inequality. \square

Theorem 6 (Stability of the WOPSIP method) *Assume that Ω is convex. For any $f \in L^2(\Omega)^d$, let $(u_h, p_h) \in V_{dc,h}^{CR} \times Q_h^0$ be the solution of (3.1). Then,*

$$|u_h|_{V_{dc,h}^{CR}} \leq \frac{C_{dc}^P}{\nu} \|f\|_{L^2(\Omega)^d}, \quad \|p_h\|_{Q_h^0} \leq \frac{2C_{dc}^P}{\beta_*} \|f\|_{L^2(\Omega)^d}, \quad (3.17)$$

where C_{dc}^P is the constant from the discrete Poincaré inequality (3.12).

Proof Setting $v_h := u_h$ in (3.1a) and $q_h := p_h$ in (3.1b) and the discrete Poincaré inequality (3.12) yields

$$\nu |u_h|_{V_{dc,h}^{CR}}^2 \leq \|f\|_{L^2(\Omega)^d} \|u_h\|_{L^2(\Omega)^d} \leq C_{dc}^P \|f\|_{L^2(\Omega)^d} |u_h|_{V_{dc,h}^{CR}},$$

which leads to the first inequality of (3.17).

For the estimate of the pressure, using the inf-sup condition (3.13), the equation (3.1a), the Hölder's inequality, the discrete Poincaré inequality (3.12), and the first inequality of (3.17) yields

$$\begin{aligned} \beta_* \|p_h\|_{Q_h^0} &\leq \sup_{v_h \in V_{dc,h}^{CR}} \frac{|b_h(v_h, p_h)|}{|v_h|_{V_{dc,h}^{CR}}} \\ &= \sup_{v_h \in V_{dc,h}^{CR}} \frac{|\int_{\Omega} f \cdot v_h dx - \nu a_h^{wop}(u_h, v_h)|}{|v_h|_{V_{dc,h}^{CR}}} \\ &\leq \sup_{v_h \in V_{dc,h}^{CR}} \frac{C_{dc}^P \|f\|_{L^2(\Omega)^d} |v_h|_{V_{dc,h}^{CR}} + \nu |u_h|_{V_{dc,h}^{CR}} |v_h|_{V_{dc,h}^{CR}}}{|v_h|_{V_{dc,h}^{CR}}} \\ &= C_{dc}^P \|f\|_{L^2(\Omega)^d} + \nu |u_h|_{V_{dc,h}^{CR}} \leq 2C_{dc}^P \|f\|_{L^2(\Omega)^d}, \end{aligned}$$

which leads to the second inequality of (3.17). \square

3.3 Error estimates of the WOPSIP method

Lemma 8 *Assume that Ω is convex. Let $(u, p) \in V \times Q$ be the solution of (2.2) and $(u_h, p_h) \in V_{dc,h}^{CR} \times Q_h^0$ be the solution of (3.1). It then holds that*

$$\begin{aligned} & |u - u_h|_{V_{dc,h}^{CR}} + \|p - p_h\|_{Q_h^0} \\ & \leq C(\beta_*) \left\{ \inf_{v_h \in V_{dc,h}^{CR}} |u - v_h|_{V_{dc,h}^{CR}} + \frac{1}{\nu} \inf_{q_h \in Q_h^0} \|p - q_h\|_{Q_h^0} + \frac{1}{\nu} E_h(u, p) \right\}, \end{aligned} \quad (3.18)$$

where

$$E_h(u, p) := \sup_{w_h \in V_{dc,h}^{CR}} \frac{|\nu a_h^{wop}(u, w_h) - \int f \cdot w_h dx + b_h(w_h, p)|}{|w_h|_{V_{dc,h}^{CR}}}. \quad (3.19)$$

Proof A proof can be similarly completed for the CR finite element approximation and standard; e.g., see [32, Lemma 14.3.1]. \square

The essential part for error estimates is the consistency error term (3.19).

Lemma 9 (Asymptotic Consistency) *Assume that Ω is convex. Let $(u, p) \in (V \cap H^2(\Omega)^d) \times (Q \cap H^1(\Omega))$ be the solution of the homogeneous Dirichlet Stokes problem (2.2) with data $f \in L^2(\Omega)^d$. Let $\{\mathbb{T}_h\}$ be a family of conformal meshes with the semi-regular property (Assumption 1). Let $T \in \mathbb{T}_h$ be the element with Conditions 1 or 2 and satisfy (Type i) in Section 2.5 when $d = 3$. Then,*

$$\begin{aligned} & E_h(u, p) \\ & \leq c\nu \left(\sum_{i,j=1}^d \sum_{T \in \mathbb{T}_h} h_j^2 \left\| \frac{\partial}{\partial r_j} \nabla u_i \right\|_{L^2(T)^d}^2 \right)^{\frac{1}{2}} + c\nu h \|\Delta u\|_{L^2(\Omega)^d} + ch \|f\|_{L^2(\Omega)^d} \\ & \quad + ch |p|_{H^1(\Omega)} + ch^{\frac{3}{2}} \|f\|_{L^2(\Omega)^d}^{\frac{1}{2}} (\nu \|\Delta u\|_{L^2(\Omega)^d} + |p|_{H^1(\Omega)})^{\frac{1}{2}}. \end{aligned} \quad (3.20)$$

Furthermore, let $d = 3$ and let T_j be the element with Condition 2 and satisfy (Type ii) in Section 2.5. It then holds that

$$E_h(u, p) \leq c\nu h \|\Delta u\|_{L^2(\Omega)^3} + ch |p|_{H^1(\Omega)} + ch \|f\|_{L^2(\Omega)^3} \quad (3.21)$$

if $|u|_{H^2(\Omega)^3} \leq c \|\Delta u\|_{L^2(\Omega)^3}$ holds.

Proof For $i = 1, \dots, d$, we first have

$$\operatorname{div}(\mathcal{I}_h^{RT}(\nu \nabla u_i - p e_i)) = \Pi_h^0 \operatorname{div}(\nu \nabla u_i - p e_i) = \Pi_h^0 \left(\nu \Delta u_i - \frac{\partial p}{\partial x_i} \right) = -\Pi_h^0 f_i,$$

where (e_1, \dots, e_d) denotes the Cartesian basis of \mathbb{R}^d .

Setting $w := \nu \nabla u_i - pe_i$ in (3.6) yields

$$\begin{aligned}
& \nu a_h^{wop}(u, w_h) - \int_{\Omega} f \cdot w_h dx + b_h(w_h, p) \\
&= \sum_{i=1}^d \left\{ \nu \int_{\Omega} (\nabla u_i - \mathcal{I}_h^{RT} \nabla u_i) \cdot \nabla_h w_{h,i} dx \right. \\
&\quad + \sum_{F \in \mathcal{F}_h^i} \int_F \{ \{ w \} \}_{\omega, F} \cdot n_F \Pi_F^0 [w_{h,i}]_F ds + \sum_{F \in \mathcal{F}_h^{\partial}} \int_F (w \cdot n_F) \Pi_F^0 w_{h,i} ds \\
&\quad \left. - \int_{\Omega} (f_i - \Pi_h^0 f_i) w_{h,i} dx + \int_{\Omega} (\mathcal{I}_h^{RT}(pe_i) - (pe_i)) \cdot \nabla_h w_{h,i} dx \right\} \\
&=: I_1 + I_2 + I_3 + I_4 + I_5.
\end{aligned}$$

Let $T \in \mathbb{T}_h$ be the element with Conditions 1 or 2 and satisfy (Type i) in Section 2.5 when $d = 3$. Using the Hölder's inequality, the Cauchy-Schwarz inequality and the RT interpolation error (2.35), the term I_1 is estimated as

$$\begin{aligned}
|I_1| &\leq c\nu \sum_{i=1}^d \sum_{T \in \mathbb{T}_h} \|\nabla u_i - \mathcal{I}_h^{RT} \nabla u_i\|_{L^2(T)} |w_{h,i}|_{H^1(T)} \\
&\leq c\nu \sum_{i=1}^d \sum_{T \in \mathbb{T}_h} \left(\sum_{j=1}^d h_j \left\| \frac{\partial}{\partial r_j} \nabla u_i \right\|_{L^2(T)^d} + h_T \|\Delta u_i\|_{L^2(T)} \right) |w_{h,i}|_{H^1(T)} \\
&\leq c\nu \left\{ \left(\sum_{i,j=1}^d \sum_{T \in \mathbb{T}_h} h_j^2 \left\| \frac{\partial}{\partial r_j} \nabla u_i \right\|_{L^2(T)^d}^2 \right)^{\frac{1}{2}} + h \|\Delta u\|_{L^2(\Omega)^s} \right\} |w_h|_{V_{dc,h}^{CR}}.
\end{aligned}$$

Using the Cauchy-Schwarz and Jensen inequalities for $a_1, a_2, a_3 \in \mathbb{R}_+$ and $b_1, b_2 \in \mathbb{R}_+ \cup \{0\}$,

$$\begin{aligned}
& \sum_{i=1}^d a_1 (a_2 + b_1)^{\frac{1}{2}} (a_3 + b_2)^{\frac{1}{2}} \\
&\leq c \left(\sum_{i=1}^d a_1^2 \right)^{\frac{1}{2}} \left\{ \left(\sum_{i=1}^d a_2^2 \right)^{\frac{1}{2}} + \left(\sum_{i=1}^d b_1^2 \right)^{\frac{1}{2}} \right\}^{\frac{1}{2}} \left\{ \left(\sum_{i=1}^d a_3^2 \right)^{\frac{1}{2}} + \left(\sum_{i=1}^d b_2^2 \right)^{\frac{1}{2}} \right\}^{\frac{1}{2}}.
\end{aligned}$$

According to the previous inequality, the triangle inequality, (2.7), (3.8) and (3.9), the terms I_2 and I_3 are estimated as

$$\begin{aligned}
|I_2| &\leq c \sum_{i=1}^d |w_{h,i}|_J \left(h \|\nu \nabla u_i - pe_i\|_{L^2(\Omega)^d} \right. \\
&\quad \left. + h^{\frac{3}{2}} \|\nu \nabla u_i - pe_i\|_{L^2(\Omega)^d}^{\frac{1}{2}} |\nu \nabla u_i - pe_i|_{H^1(\Omega)^d}^{\frac{1}{2}} \right)
\end{aligned}$$

$$\begin{aligned}
&\leq c \sum_{i=1}^d |w_{h,i}|_J \left\{ h(\nu|u_i|_{H^1(\Omega)} + \|pe_i\|_{L^2(\Omega)^d}) \right. \\
&\quad \left. + h^{\frac{3}{2}}(\nu|u_i|_{H^1(\Omega)} + \|pe_i\|_{L^2(\Omega)^d})^{\frac{1}{2}}(\nu\|\Delta u_i\|_{L^2(\Omega)} + |p|_{H^1(\Omega)})^{\frac{1}{2}} \right\} \\
&\leq c|w_h|_{V_{dc,h}^{CR}} \left\{ h(\nu|u|_{H^1(\Omega)^d} + \|p\|_{L^2(\Omega)}) \right. \\
&\quad \left. + h^{\frac{3}{2}}(\nu|u|_{H^1(\Omega)^d} + \|p\|_{L^2(\Omega)})^{\frac{1}{2}}(\nu\|\Delta u\|_{L^2(\Omega)^d} + |p|_{H^1(\Omega)})^{\frac{1}{2}} \right\} \\
&\leq c|w_h|_{V_{dc,h}^{CR}} \left\{ h\|f\|_{L^2(\Omega)^d} + h^{\frac{3}{2}}\|f\|_{L^2(\Omega)^d}^{\frac{1}{2}}(\nu\|\Delta u\|_{L^2(\Omega)^d} + |p|_{H^1(\Omega)})^{\frac{1}{2}} \right\}, \\
|I_3| &\leq c|w_h|_{V_{dc,h}^{CR}} \left\{ h\|f\|_{L^2(\Omega)^d} + h^{\frac{3}{2}}\|f\|_{L^2(\Omega)^d}^{\frac{1}{2}}(\nu\|\Delta u\|_{L^2(\Omega)^d} + |p|_{H^1(\Omega)})^{\frac{1}{2}} \right\}.
\end{aligned}$$

Using the Hölder's inequality, the Cauchy–Schwarz inequality, the stability of Π_h^0 and the estimate (2.16), the term I_4 is estimated as

$$\begin{aligned}
|I_4| &= \left| \sum_{i=1}^d \int_{\Omega} (f_i - \Pi_h^0 f_i) (w_{h,i} - \Pi_h^0 w_{h,i}) dx \right| \\
&\leq \sum_{i=1}^d \sum_{T \in \mathbb{T}_h} \|f_i - \Pi_h^0 f_i\|_{L^2(T)} \|w_{h,i} - \Pi_h^0 w_{h,i}\|_{L^2(T)} \\
&\leq ch\|f\|_{L^2(\Omega)^d} |w_h|_{V_{dc,h}^{CR}}.
\end{aligned}$$

Using the Hölder's inequality, the Cauchy–Schwarz inequality and the RT interpolation error (2.35), the term I_5 is estimated as

$$\begin{aligned}
|I_5| &\leq \sum_{i=1}^d \sum_{T \in \mathbb{T}_h} \|\mathcal{I}_h^{RT}(pe_i) - (pe_i)\|_{L^2(\Omega)} |w_{h,i}|_{H^1(T)} \\
&\leq c \sum_{i=1}^d \sum_{T \in \mathbb{T}_h} \left(\sum_{j=1}^d h_j \left\| \frac{\partial(pe_i)}{\partial r_j} \right\|_{L^2(T)^d} + h_T \|\operatorname{div}(pe_i)\|_{L^2(T)} \right) |w_{h,i}|_{H^1(T)} \\
&\leq c \left\{ \left(\sum_{j=1}^d \sum_{T \in \mathbb{T}_h} h_j^2 \left\| \frac{\partial p}{\partial r_j} \right\|_{L^2(T)}^2 \right)^{\frac{1}{2}} + h|p|_{H^1(\Omega)} \right\} |w_h|_{V_{dc,h}^{CR}} \\
&\leq ch|p|_{H^1(\Omega)} |w_h|_{V_{dc,h}^{CR}}.
\end{aligned}$$

Gathering the above inequalities yields the target inequality (3.20).

Let $d = 3$ and let T_j be the element with Condition 2 and satisfy (Type ii) in Section 2.5. Using the Hölder's inequality, the Cauchy–Schwarz inequality

and the RT interpolation error (2.36), the terms I_1 and I_5 are estimated as

$$\begin{aligned} |I_1| &\leq c\nu h|u|_{H^2(\Omega)^3}|w_h|_{V_{dc,h}^{CR}}, \\ |I_5| &\leq ch|p|_{H^1(\Omega)}|w_h|_{V_{dc,h}^{CR}}, \end{aligned}$$

which implies the target inequality (3.21). \square

Theorem 7 (Error Estimate) *Assume that Ω is convex. Let $(u, p) \in (V \cap H^2(\Omega)^d) \times (Q \cap H^1(\Omega))$ be the solution to the homogeneous Dirichlet problem for the Stokes equation (2.2) with data $f \in L^2(\Omega)^d$. Let $\{\mathbb{T}_h\}$ be a family of conformal meshes with the semi-regular property (Assumption 1). Let $T \in \mathbb{T}_h$ be the element with Conditions 1 or 2 and satisfy (Type i) in Section 2.5 when $d = 3$. Then,*

$$\begin{aligned} &|u - u_h|_{V_{dc,h}^{CR}} + \|p - p_h\|_{Q_h^0} \\ &\leq c \left(\sum_{i,j=1}^d \sum_{T \in \mathbb{T}_h} h_j^2 \left\| \frac{\partial}{\partial r_j} \nabla u_i \right\|_{L^2(T)^d}^2 \right)^{\frac{1}{2}} + ch \|\Delta u\|_{L^2(\Omega)^d} + c \frac{h}{\nu} \|f\|_{L^2(\Omega)^d} \\ &\quad + c \frac{h}{\nu} |p|_{H^1(\Omega)} + c \frac{h^{\frac{3}{2}}}{\nu} \|f\|_{L^2(\Omega)^d}^{\frac{1}{2}} (\nu \|\Delta u\|_{L^2(\Omega)^d} + |p|_{H^1(\Omega)})^{\frac{1}{2}}. \end{aligned} \quad (3.22)$$

Furthermore, let $d = 3$ and let T_j be the element with Condition 2 and satisfy (Type ii) in Section 2.5. Then

$$\begin{aligned} &|u - u_h|_{V_{dc,h}^{CR}} + \|p - p_h\|_{Q_h^0} \\ &\leq ch \|\Delta u\|_{L^2(\Omega)^3} + c \frac{h}{\nu} |p|_{H^1(\Omega)} + c \frac{h}{\nu} \|f\|_{L^2(\Omega)^3} \end{aligned} \quad (3.23)$$

if $|u|_{H^2(\Omega)^3} \leq c \|\Delta u\|_{L^2(\Omega)^3}$ holds.

Proof Using the definition of the L^2 -projection Π_F^0 and the definition of $\mathcal{I}_h^{CR}v$, for $i = 1, \dots, d$, we have

$$\begin{aligned} \|\Pi_F^0 \llbracket (\mathcal{I}_h^{CR}v)_i - v_i \rrbracket\|_{L^2(F)}^2 &= \int_F \Pi_F^0 \llbracket (\mathcal{I}_h^{CR}v)_i - v_i \rrbracket \Pi_F^0 \llbracket (\mathcal{I}_h^{CR}v)_i - v_i \rrbracket ds \\ &= \int_F \llbracket (\mathcal{I}_h^{CR}v)_i - v_i \rrbracket \Pi_F^0 \llbracket (\mathcal{I}_h^{CR}v)_i - v_i \rrbracket ds = 0. \end{aligned} \quad (3.24)$$

Therefore, using (2.27) and (3.24), we obtain

$$\begin{aligned} \inf_{v_h \in V_{dc,h}^{CR}} |u - v_h|_{V_{dc,h}^{CR}} &\leq |u - \mathcal{I}_h^{CR}u|_{V_{dc,h}^{CR}} = |u - \mathcal{I}_h^{CR}u|_{H^1(\mathbb{T}_h)^d} \\ &\leq c \left(\sum_{i,j=1}^d \sum_{T \in \mathbb{T}_h} h_j^2 \left\| \frac{\partial}{\partial r_j} \nabla u_i \right\|_{L^2(T)^d}^2 \right)^{\frac{1}{2}} \end{aligned} \quad (3.25)$$

$$\leq ch|u|_{H^2(\Omega)^d}. \quad (3.26)$$

The estimate (2.16) yields

$$\begin{aligned} \inf_{q_h \in Q_h^0} \|p - q_h\|_{Q_h^0} &\leq \|p - \Pi_h^0 p\|_{Q_h^0} \\ &\leq c \left(\sum_{j=1}^d \sum_{T \in \mathbb{T}_h} h_j^2 \left\| \frac{\partial p}{\partial r_j} \right\|_{L^2(T)}^2 \right)^{\frac{1}{2}} \leq ch|p|_{H^1(\Omega)}. \end{aligned} \quad (3.27)$$

From (3.18), (3.20), (3.25) and (3.27), we conclude by deriving the desired inequality (3.22).

The estimate (3.23) is deduced from (3.18), (3.21), (3.26) and (3.27). \square

4 Numerical experiments

Let $d = 2$ and $\Omega := (0, 1)^2$.

4.1 Comparison of calculations for some schemes on anisotropic meshes

In this section, we present numerical tests for some schemes on anisotropic meshes. We set $\varphi(x_1, x_2) := x_1^2(x_1 - 1)^2 x_2^2(x_2 - 1)^2$. The function f of the Stokes equation (2.1) with $\nu = 1$,

$$-\Delta u + \nabla p = f \quad \text{in } \Omega, \quad \operatorname{div} u = 0 \quad \text{in } \Omega, \quad u = 0 \quad \text{on } \partial\Omega,$$

is given so that the exact solution is

$$\begin{aligned} \begin{pmatrix} u_1 \\ u_2 \end{pmatrix} &= \begin{pmatrix} \frac{\partial \varphi}{\partial x_2} \\ -\frac{\partial \varphi}{\partial x_1} \end{pmatrix} = \begin{pmatrix} 2x_1^2(x_1 - 1)^2 x_2(x_2 - 1)^2 + 2x_1^2(x_1 - 1)^2 x_2^2(x_2 - 1) \\ -2x_1(x_1 - 1)^2 x_2^2(x_2 - 1)^2 - 2x_1^2(x_1 - 1)x_2^2(x_2 - 1)^2 \end{pmatrix}, \\ p &= x_1^2 - x_2^2. \end{aligned}$$

Let $N \in \{32, 64\}$ be the division number of each side of the bottom and the height edges of Ω . We consider four types of mesh partitions. Let $(x_1^i, x_2^i)^T$ be grip points of triangulations \mathbb{T}_h defined as follows. Let $i \in \mathbb{N}$.

(I) Standard mesh (Fig. 1)

$$x_1^i := \frac{i}{N}, \quad x_2^i := \frac{i}{N}, \quad i \in \{0, \dots, N\}.$$

(II) Shishkin mesh (Fig. 2)

$$\begin{aligned} x_1^i &:= \frac{i}{N}, \quad i \in \{0, \dots, N\}, \\ x_2^i &:= \begin{cases} \tau \frac{2}{N} i, & i \in \{0, \dots, \frac{N}{2}\}, \\ \tau + (1 - \tau) \frac{2}{N} (i - \frac{N}{2}), & i \in \{\frac{N}{2} + 1, \dots, N\}, \end{cases} \end{aligned}$$

where $\tau := 4\delta |\ln(N)|$ with $\delta = \frac{1}{128}$, see [43, Section 2.1.2].

(III) Anisotropic mesh from [18] (Fig. 3)

$$x_1^i := \frac{i}{N}, \quad x_2^i := \frac{1}{2} \left(1 - \cos \left(\frac{i\pi}{N} \right) \right), \quad i \in \{0, \dots, N\}.$$

(IV) Anisotropic mesh (Fig. 4)

$$x_1^i := \frac{i}{N}, \quad x_2^i := \left(\frac{i}{N} \right)^2, \quad i \in \{0, \dots, N\}.$$

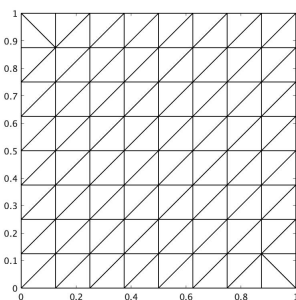


Fig. 1: (I) Standard mesh

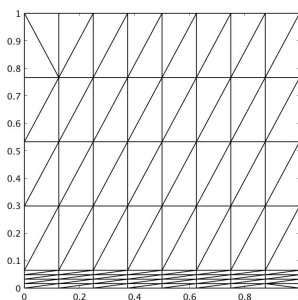


Fig. 2: (II) Shishkin mesh, $\delta = \frac{1}{128}$

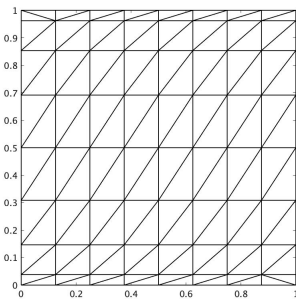


Fig. 3: (III) Anisotropic mesh

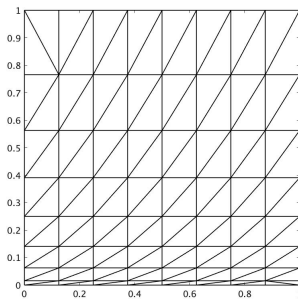


Fig. 4: (IV) Anisotropic mesh

The shape-regularity condition is known: there exists a constant $\gamma_1 > 0$ such that

$$\rho_T \geq \gamma_1 h_T \quad \forall \mathbb{T}_h \in \{\mathbb{T}_h\}, \quad \forall T \in \mathbb{T}_h,$$

and is equivalent to the following condition. There exists a constant $\gamma_2 > 0$ such that for any $\mathbb{T}_h \in \{\mathbb{T}_h\}$ and simplex $T \in \mathbb{T}_h$, we have

$$|T|_2 \geq \gamma_2 h_T^2.$$

A proof is provided in [12, Theorem 1]. The semiregularity mesh condition defined in (2.15) is equivalent to the maximum angle condition. The following parameters are computed.

$$\text{MinAngle} := \max_{T \in \mathbb{T}_h} \frac{|L_3|_1^2}{|T|_2}, \quad \text{MaxAngle} := \max_{T \in \mathbb{T}_h} \frac{|L_1|_1 |L_2|_1}{|T|_2},$$

where L_i , $i = 1, 2, 3$, denote the edges of the simplex $T \in \mathbb{T}_h$ with $|L_1|_1 \leq |L_2|_1 \leq |L_3|_1$.

Table 1: Mesh conditions

Mesh	N	MinAngle	MaxAngle
I	32	4.00000	2.00000
	64	4.00000	2.00000
II	32	9.66647	2.00000
	64	8.21423	2.00000
III	32	2.61132e+01	2.00000
	64	5.19640e+01	2.00000
IV	32	6.40625e+01	2.00000
	64	1.28031e+02	2.00000

Notably, a sequence with meshes (I) or (II) satisfies the shape-regularity condition, but a sequence with meshes (III), or (IV) does not satisfy the shape regularity condition.

We adopt the following schemes.

- (1) Scheme (3.1).
- (2) Hybrid dG (HdG) method with a penalty term. Let $k \in \mathbb{N}$. We define a discrete space as $A_h^k := \{\lambda_h \in L^2(\mathcal{F}_h)^2 : \lambda_h|_F \in \mathbb{P}^k(F)^2 \forall F \in \mathcal{F}_h, \lambda_h|_{\partial\Omega} = 0\}$. Find $(u_h, \lambda_h, p_h) \in V_{dc,h}^k \times A_h^k \times P_{dc,h}^{k-1}$ such that

$$a_h^{\text{HdG}}(u_h, \lambda_h; v_h, \mu_h) + b_h^{\text{HdG}}(v_h, \mu_h; p_h) = \int_{\Omega} f \cdot v_h dx \quad \forall (v_h, \mu_h) \in V_{dc,h}^k \times A_h^k, \quad (4.1a)$$

$$b_h^{\text{HdG}}(u_h, \lambda_h; q_h) - 10^{-10} \int_{\Omega} p_h q_h dx = 0 \quad \forall q_h \in P_{dc,h}^{k-1}, \quad (4.1b)$$

where

$$\begin{aligned}
a_h^{HdG}(u_h, \lambda_h; v_h, \mu_h) &:= \int_{\Omega} \nabla_h u_h : \nabla_h v_h dx \\
&+ \sum_{T \in \mathbb{T}_h} \sum_{F \in \mathcal{F}_T} \frac{\eta}{h_F} \int_F (\lambda_h - u_h) \cdot (\mu_h - v_h) ds \\
&+ \sum_{T \in \mathbb{T}_h} \int_{\partial T} (\nabla_h u_h n_F \cdot (\mu_h - v_h) + (\lambda_h - u_h) \cdot \nabla_h v_h n_F) ds, \\
b_h^{HdG}(v_h, \mu_h; q_h) &:= - \int_{\Omega} \operatorname{div}_h v_h q_h dx - \sum_{T \in \mathbb{T}_h} \int_{\partial T} (\mu_h - v_h) \cdot n_F q_h ds,
\end{aligned}$$

for any $(u_h, \lambda_h) \in V_{dc,h}^k \times \Lambda_h^k$, $(v_h, \mu_h) \in V_{dc,h}^k \times \Lambda_h^k$, and $q_h \in P_{dc,h}^{k-1}$. Here, η is a positive real number.

- (3) Conforming finite element method with a penalty parameter. Let $k \in \mathbb{N}$. We define discrete spaces as $P_{c,h}^k := \{p_h \in H^1(\Omega); p_h|_T \in \mathbb{P}^k(T) \forall T \in \mathbb{T}_h\}$, and $V_{c,h}^2 := (P_{c,h}^2 \cap H_0^1(\Omega))^2$. Find $(u_h, p_h) \in V_{c,h}^2 \times P_{c,h}^1$ such that

$$a_h^c(u_h, v_h) + b_h^c(v_h, p_h) = \int_{\Omega} f \cdot v_h dx \quad \forall v_h \in V_{c,h}^2, \quad (4.2a)$$

$$b_h^c(u_h, q_h) - 10^{-10} \int_{\Omega} p_h q_h dx = 0 \quad \forall q_h \in P_{c,h}^1, \quad (4.2b)$$

where

$$a_h^c(u_h, v_h) := \int_{\Omega} \nabla u_h : \nabla v_h dx, \quad b_h^c(v_h, q_h) := - \int_{\Omega} \operatorname{div} v_h q_h dx,$$

for any $u_h \in V_{c,h}^2$, $v_h \in V_{c,h}^2$, and $q_h \in P_{c,h}^1$.

Remark 6 The original HdG method by [21] is as follows. Find $(u_h, \lambda_h, p_h) \in V_h^k \times \Lambda_h^k \times Q_h^{k-1}$ such that

$$a_h^{HdG}(u_h, \lambda_h; v_h, \mu_h) + b_h^{HdG}(v_h, \mu_h; p_h) = \int_{\Omega} f \cdot v_h dx \quad \forall (v_h, \mu_h) \in V_h^k \times \Lambda_h^k, \quad (4.3a)$$

$$b_h^{HdG}(u_h, \lambda_h; q_h) = 0 \quad \forall q_h \in Q_h^{k-1}, \quad (4.3b)$$

where the terms a_h^{HdG} and b_h^{HdG} are as defined above.

If an exact solution u is known, the error $e_h := u - u_h$ and $e_{h/2} := u - u_{h/2}$ are computed numerically for two mesh sizes h and $h/2$. The convergence indicator r is defined by

$$r = \frac{1}{\log(2)} \log \left(\frac{\|e_h\|_X}{\|e_{h/2}\|_X} \right).$$

We compute the convergence order with respect to norms defined by

$$E_{u_h}^{(\text{Mesh No.})} := \frac{|u - u_h|_{V_{dc,h}^{CR}}}{|u|_{H^1(\Omega)^2}} \quad \text{for scheme (1),}$$

$$E_{u_h}^{(\text{Mesh No.})} := \frac{|u - u_h|_{H^1(\mathbb{T}_h)^2}}{|u|_{H^1(\Omega)^2}}$$

for schemes (2), (3), and the WBCR method,

$$E_{u_h, L^2}^{(\text{Mesh No.})} := \frac{\|u - u_h\|_{L^2(\Omega)^2}}{\|u\|_{L^2(\Omega)^2}}, \quad E_{p_h}^{(\text{Mesh No.})} := \frac{\|p - p_h\|_{L^2(\Omega)}}{\|p\|_{L^2(\Omega)}}.$$

For the computation of scheme (1), we used the CG method without preconditioners, and the quadrature of the five order for computation of the right-hand side in (3.1a), see [24, p. 85, Table 30.1]. For the computation of the schemes (2), and (3), we used the FreeFEM software tool [31,29] based on code provided in the prior work [44] and used UMFPACK.

Table 2: Scheme (1)

Mesh	N	$E_{u_h}^{(\text{Mesh No.})}$	r	$E_{u_h, L^2}^{(\text{Mesh No.})}$	r	$E_{p_h}^{(\text{Mesh No.})}$	r
I	32	8.10569e-01		2.12630e-01		3.61598e-02	
	64	4.08981e-01	0.99	5.42357e-02	1.97	1.35562e-02	1.42
II	32	1.15924		4.33629e-01		6.52059e-02	
	64	5.79411e-01	1.00	1.08800e-01	1.99	2.22654e-02	1.55
III	32	1.05163		3.60039e-01		5.24322e-02	
	64	5.34097e-01	0.98	9.31283e-02	1.95	1.76734e-02	1.57
IV	32	1.23942		4.97459e-01		7.17788e-02	
	64	6.36438e-01	0.96	1.31655e-01	1.92	2.44549e-02	1.55

Table 3: Scheme (2) with $k = 1$

Mesh	N	η	$E_{u_h}^{(\text{Mesh No.})}$	r	$E_{u_h, L^2}^{(\text{Mesh No.})}$	r	$E_{p_h}^{(\text{Mesh No.})}$	r
I	32	20	7.65762e-02		6.54741e-03		2.35152e-02	
	64	20	3.74884e-02	1.03	1.60004e-03	2.03	1.14994e-02	1.03
II	32	30	1.08934e-01		1.27498e-02		3.78265e-02	
	64	30	4.50132e-02	1.28	3.03009e-03	2.07	1.84420e-02	1.04
III	32	40	8.22514e-02		1.01627e-02		2.92376e-02	
	64	40	3.88132e-02	1.08	2.50863e-03	2.02	1.44096e-02	1.02
IV	32	40	9.87191e-02		1.34999e-02		3.86220e-02	
	64	40	4.60525e-02	1.10	3.34145e-03	2.01	1.90213e-02	1.02

The tables 2, 3, and 4 imply that the inf-sup condition is satisfied on anisotropic meshes. However, to the best of our knowledge, a theoretical analysis of the HdG method on anisotropic meshes has not been considered in the relevant literature. Furthermore, one needs to tune up the parameter η . The

Table 4: Scheme (2) with $k = 2$

Mesh	N	η	$E_{u_h}^{(\text{Mesh No.})}$	r	$E_{u_h, L^2}^{(\text{Mesh No.})}$	r	$E_{p_h}^{(\text{Mesh No.})}$	r
I	32	20	2.66367e-03		5.34649e-05		1.61446e-04	
	64	20	6.65586e-04	2.00	6.72505e-06	2.99	4.03072e-05	2.00
II	32	20	7.45375e-03		1.79222e-04		3.96913e-04	
	64	40	1.00195e-03	2.90	1.98821e-05	3.17	1.01078e-04	1.97
III	32	20	6.37078e-03		9.19734e-05		2.59598e-04	
	64	40	7.54222e-04	3.08	1.06225e-05	3.11	7.90454e-05	1.72
IV	32	30	5.47512e-03		1.47191e-04		3.58253e-04	
	64	60	1.11295e-03	2.30	1.95215e-05	2.91	1.44366e-04	1.31

Table 5: Scheme (3)

Mesh	N	$E_{u_h}^{(\text{Mesh No.})}$	r	$E_{u_h, L^2}^{(\text{Mesh No.})}$	r	$E_{p_h}^{(\text{Mesh No.})}$	r
I	32	2.86851e-03		8.51503e-05		2.44204e-04	
	64	7.18451e-04	2.00	1.06518e-05	3.00	6.09198e-05	2.00
II	32	5.11492e-03		2.31144e-04		5.25401e-04	
	64	1.19256e-03	2.10	2.66944e-05	3.11	1.10624e-04	2.25
III	32	3.35828e-03		1.19972e-04		3.56077e-04	
	64	8.41989e-04	2.00	1.50243e-05	3.00	8.89802e-05	2.00
IV	32	4.60495e-03		2.02053e-04		4.35519e-04	
	64	1.16069e-03	1.99	2.52328e-05	3.00	1.08824e-04	2.00

table 5 also implies that the inf-sup condition is satisfied on anisotropic meshes. The inf-sup condition in two-dimensional cases is proven in the previous work [9].

4.2 Penalty parameters

One disadvantage of the WOPSIP method is that it increases the number of conditions. In particular, the penalty parameter κ_F increases as $h \rightarrow 0$. On the mesh (II), we compute the following qualities (Table 6).

$$\tau_{\max}^{(f)} := \max_{F \in \mathcal{F}_h^i} \frac{1}{h_F}, \quad \tau_{\max}^{(ave)} := \max_{F \in \mathcal{F}_h^i} \frac{1}{4} \left(\frac{1}{\ell_{T_1, F}} + \frac{1}{\ell_{T_2, F}} \right),$$

$$\tau_{\max}^{(dg)} := \max_{F \in \mathcal{F}_h^i} \frac{2}{(\sqrt{\ell_{T_1, F}} + \sqrt{\ell_{T_2, F}})^2}, \quad \tau_{\max}^{(wop)} := \max_{F \in \mathcal{F}_h^i} \frac{2}{h^2 (\sqrt{\ell_{T_1, F}} + \sqrt{\ell_{T_2, F}})^2}$$

Table 6 shows that the penalty parameter of the WOPSIP method is considerably larger than the others. The problem of the ill-conditioning on anisotropic meshes is left for future research. The improvement of the ill-conditioning for the Poisson equation is stated in [15].

Table 6: Comparison of penalty parameters: Mesh (II): $\delta = \frac{1}{1024}$

N	$1/h$	$\tau_{\max}^{(f)}$	$\tau_{\max}^{(ave)}$	$\tau_{\max}^{(dg)}$	$\tau_{\max}^{(wop)}$
16	7.2179e+00	7.3866e+02	3.6942e+02	3.6942e+02	1.9246e+04
32	1.4467e+01	1.1819e+03	5.9114e+02	5.9114e+02	1.2373e+05
64	2.8998e+01	1.9698e+03	9.8540e+02	9.8540e+02	8.2860e+05
128	5.8123e+01	3.3767e+03	1.6896e+03	1.6896e+03	5.7079e+06
256	1.1650e+02	5.9093e+03	2.9574e+03	2.9574e+03	4.0139e+07

4.3 Comparison of the penalty parameters

Numerical calculations for the problem in Section 4.1 were performed using the parameter κ_{F^*} instead of the parameter κ_F for scheme (3.1). The convergence order was computed with respect to the norms defined by

$$E_h^{(\text{Mesh No.})} := \frac{|u - u_h|_{V_{dc,h}^{CR}} + \|p - p_h\|_{L^2(\Omega)}}{|u|_{H^1(\Omega)^2} + \|p\|_{L^2(\Omega)}}.$$

Table 7 presents the numerical results obtained using Mesh (I). The case that uses parameter κ_{F^*} is unlikely to converge.

Table 7: WOPSIP method with κ_F, κ_{F^*}

N	$\#Np$	h	$E_h^{(I)}(\kappa_F)$	r	$E_h^{(I)}(\kappa_{F^*})$	r
16	3,584	8.84e-02	2.81448e-01		1.81628	
32	14,336	4.42e-02	1.28586e-01	1.13	1.81324	-
64	57,344	2.21e-02	6.07505e-02	1.08	1.81236	-
128	229,376	1.10e-02	2.97281e-02	1.03	1.81213	-
256	917,504	5.52e-03	1.47711e-02	1.01	1.81207	-

4.4 Comparison with the well-balanced CR method

We set $\varphi(x_1, x_2) := x_1^2(x_1 - 1)^2 x_2^2(x_2 - 1)^2 \exp\left(-\frac{x_2}{\eta}\right)$ with $\eta := \sqrt{\delta}$ and $\delta \in \left\{\frac{1}{64}, \frac{1}{128}, \frac{1}{256}\right\}$. The function f of the Stokes equation (2.1) with $\nu = 1$ is given so that the exact solution is

$$\begin{pmatrix} u_1 \\ u_2 \end{pmatrix} = \begin{pmatrix} \frac{\partial \varphi}{\partial x_2} \\ -\frac{\partial \varphi}{\partial x_1} \end{pmatrix}, \quad p = x_1^2(x_1 - 1)^2 \exp\left(-\frac{x_2}{\delta}\right) - \frac{\delta}{30} + \frac{\delta}{30} \exp\left(-\frac{1}{\delta}\right).$$

Note that $\int_{\Omega} p dx \approx 0$. See Fig. 5.

Remark 7 Through a simple calculation,

$$\begin{aligned}\frac{\partial^2 u_1}{\partial x_2^2} &= \left(-\frac{1}{\eta^3} x_1^2 (x_1 - 1)^2 x_2^2 (x_2 - 1)^2 + C_1(x_1, x_2, \eta) \right) \exp\left(-\frac{x_2}{\eta}\right), \\ \frac{\partial^2 u_2}{\partial x_2^2} &= -\frac{2}{\eta^2} (x_1(x_1 - 1)^2 + x_1^2(x_1 - 1)) x_2^2 (x_2 - 1)^2 \exp\left(-\frac{x_2}{\eta}\right) \\ &\quad + C_2(x_1, x_2, \eta) \exp\left(-\frac{x_2}{\eta}\right), \\ \frac{\partial p}{\partial x_2} &= -\frac{1}{\delta} x_1^2 (x_1 - 1)^2 \exp\left(-\frac{x_2}{\delta}\right),\end{aligned}$$

where $C_1(x_1, x_2, \eta)$ and $C_2(x_1, x_2, \eta)$ are functions. In this numerical experiment, we set $\eta = \sqrt{\delta}$.

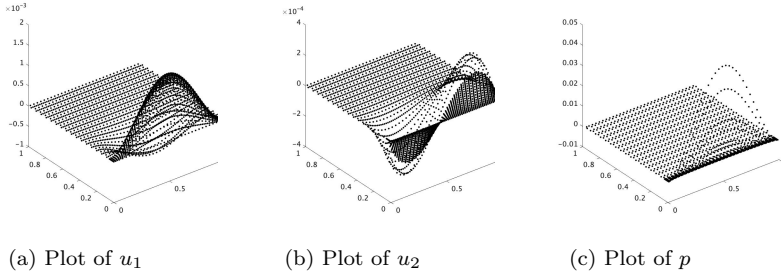


Fig. 5: Mesh (II) Plot of the exact solution, $\eta = \frac{1}{16}$, $\delta = \frac{1}{256}$

In the computation, the following schemes were used:

- (1) Scheme (3.1) (WOPSIP method).
- (4) Well-balanced CR (WBCR) method ([42]). We define the classical RT finite element space as

$$V_{c,h}^{RT} := \{v_h \in V_{dc,h}^{RT} : \llbracket v_h \cdot n \rrbracket_F = 0, \forall F \in \mathcal{F}_h\}.$$

Let $\mathcal{I}_h^{RTc} : V_{h0}^{CR} \rightarrow V_{c,h}^{RT}$ be a classical RT interpolation operator. Find $(u_h, p_h) \in V_{h0}^{CR} \times Q_h^0$ such that

$$a_h^{CR}(u_h, v_h) + b_h^{CR}(v_h, p_h) = \int_{\Omega} f \cdot \mathcal{I}_h^{RTc} v_h dx \quad \forall v_h \in V_{h0}^{CR}, \quad (4.4a)$$

$$b_h^{CR}(u_h, q_h) = 0 \quad \forall q_h \in Q_h^0, \quad (4.4b)$$

where

$$\begin{aligned}a_h^{CR}(u_h, v_h) &:= \sum_{i=1}^d \int_{\Omega} \nabla_h u_{h,i} \cdot \nabla_h v_{h,i} dx, \\ b_h^{CR}(v_h, q_h) &:= - \int_{\Omega} \operatorname{div}_h v_h q_h dx,\end{aligned}$$

for $u_h, v_h \in V_{h0}^{CR}$ and $q_h \in Q_h^0$. Recall that space V_{h0}^{CR} was defined in Remark 5.

Let $N \in \{16, 32, 64, 128, 256\}$ be the division number for each side of the bottom and height edges of Ω . We consider meshes (I) and (II) with $\delta \in \{\frac{1}{64}, \frac{1}{128}, \frac{1}{256}\}$. The notation $\#Np$ denotes the number of nodal points on $V_{dc,h}^{CR} \times Q_h^0$ or $V_{h0}^{CR} \times Q_h^0$ including nodal points on the boundary. We further use the CG method without preconditioners and the quadrature of the five orders for the computation of the right-hand side in (3.1a) and (4.4a).

Table 8: Mesh (I) WOPSIP method, $\eta = \frac{1}{8}$, $\delta = \frac{1}{64}$

N	$\#Np$	h	$E_{u_h}^{(I)}$	r	$E_{p_h}^{(I)}$	r
16	3,584	8.84e-02	6.84774e-01		8.83176e-01	
32	14,336	4.42e-02	3.81183e-01	0.85	5.23969e-01	0.75
64	57,344	2.21e-02	1.98511e-01	0.94	2.72238e-01	0.94
128	229,376	1.10e-02	1.00464e-01	0.98	1.37158e-01	0.99
256	917,504	5.52e-03	5.03923e-02	1.00	6.86957e-02	1.00

Table 9: Mesh (II) WOPSIP method, $\eta = \frac{1}{8}$, $\delta = \frac{1}{64}$

N	$\#Np$	h	$E_{u_h}^{(I)}$	r	$E_{p_h}^{(I)}$	r
16	3,584	8.84e-02	4.99659e-01		6.39849e-01	
32	14,336	4.42e-02	2.66696e-01	0.91	3.41427e-01	0.91
64	57,344	2.21e-02	1.42234e-01	0.91	1.83575e-01	0.90
128	229,376	1.10e-02	7.58869e-02	0.91	9.90536e-02	0.89
256	917,504	5.52e-03	4.04865e-02	0.91	5.34495e-02	0.89

Table 10: Mesh (I) WOPSIP method, $\eta = \frac{1}{8\sqrt{2}}$, $\delta = \frac{1}{128}$

N	$\#Np$	h	$E_{u_h}^{(I)}$	r	$E_{p_h}^{(I)}$	r
16	3,584	8.84e-02	8.23155e-01		1.05497	
32	14,336	4.42e-02	4.89480e-01	0.75	8.08138e-01	0.38
64	57,344	2.21e-02	2.70311e-01	0.86	4.90630e-01	0.72
128	229,376	1.10e-02	1.41134e-01	0.94	2.57758e-01	0.93
256	917,504	5.52e-03	7.15209e-02	0.98	1.30291e-01	0.98

Tables 8 - 13 represent numerical results of the WOPSIP method for $\delta = \frac{1}{64}, \frac{1}{128}, \frac{1}{256}$, respectively. Tables 14 - 19 represent numerical results of the WBCR method for $\delta = \frac{1}{64}, \frac{1}{128}, \frac{1}{256}$, respectively. The WBCR method showed a trend similar to that of the WOPSIP method. We observe that the use of the Shishkin mesh (II) with the parameter $\tau = 4\delta \ln(N)$ near the bottom is likely to achieve the optimal convergence order, whereas Tables 12 and

Table 11: Mesh (II) WOPSIP method, $\eta = \frac{1}{8\sqrt{2}}$, $\delta = \frac{1}{128}$

N	$\#Np$	h	$E_{u_h}^{(II)}$	r	$E_{p_h}^{(II)}$	r
16	3,584	1.30e-01	5.97426e-01		9.36325e-01	
32	14,336	6.39e-02	3.13359e-01	0.93	4.83980e-01	0.95
64	57,344	3.14e-02	1.62259e-01	0.95	2.51145e-01	0.95
128	229,376	1.54e-02	8.35607e-02	0.96	1.30872e-01	0.94
256	917,504	7.55e-03	4.30401e-02	0.96	6.83930e-02	0.94

Table 12: Mesh (I) WOPSIP method, $\eta = \frac{1}{16}$, $\delta = \frac{1}{256}$

N	$\#Np$	h	$E_{u_h}^{(I)}$	r	$E_{p_h}^{(I)}$	r
16	3,584	8.84e-02	9.50427e-01		1.12990	
32	14,336	4.42e-02	6.04935e-01	0.65	9.94423e-01	0.18
64	57,344	2.21e-02	3.49110e-01	0.79	7.71574e-01	0.37
128	229,376	1.10e-02	1.94504e-01	0.84	4.72726e-01	0.71
256	917,504	5.52e-03	1.02293e-01	0.93	2.49118e-01	0.92

Table 13: Mesh (II) WOPSIP method, $\eta = \frac{1}{16}$, $\delta = \frac{1}{256}$

N	$\#Np$	h	$E_{u_h}^{(II)}$	r	$E_{p_h}^{(II)}$	r
16	3,584	1.35e-01	7.89295e-01		1.46492	
32	14,336	6.69e-02	4.10272e-01	0.94	7.48414e-01	0.97
64	57,344	3.31e-02	2.11273e-01	0.96	3.81425e-01	0.97
128	229,376	1.64e-02	1.07657e-01	0.97	1.94667e-01	0.97
256	917,504	8.13e-03	5.45969e-02	0.98	9.95082e-02	0.97

Table 14: Mesh (I) WBCR method, $\eta = \frac{1}{8}$, $\delta = \frac{1}{64}$

N	$\#Np$	h	$E_{u_h}^{(I)}$	r	$E_{p_h}^{(I)}$	r
16	3,584	8.84e-02	9.81333e-01		1.38484	
32	14,336	4.42e-02	5.23575e-01	0.91	6.14362e-01	1.17
64	57,344	2.21e-02	2.65825e-01	0.98	2.84631e-01	1.11
128	229,376	1.10e-02	1.33413e-01	0.99	1.38739e-01	1.04
256	917,504	5.52e-03	6.67689e-02	1.00	6.88943e-02	1.01

18 show that the mesh needs to be split sufficiently to obtain the optimum convergence order on the standard mesh (I). These demonstrate the effectiveness of the anisotropic meshes.

We illustrate approximate solutions for the boundary layer problem can be found below (Figure 6 - Figure 11) when Mesh (II), $N = 32$ and $\delta = \frac{1}{64}, \frac{1}{128}, \frac{1}{256}$. Even from the perspective of approximate solutions, it can be observed that numerical oscillations are occurring in $u_{h,2}$ and p_h in both methods. However, the oscillations of the WBCR method seem to be small. Furthermore, it can be observed that the oscillations do not spread throughout the domain. Numerical oscillations seem inevitable even if the Shishkin mesh is used. These results imply that other techniques may be needed to reduce unnatural plots near the boundary layer for approximate solutions in Navier–Stokes equations (e.g., [22, Section 3.5], [48]).

Table 15: Mesh (II) WBCR method, $\eta = \frac{1}{8}$, $\delta = \frac{1}{64}$

N	$\#N_p$	h	$E_{u_h}^{(I)}$	r	$E_{p_h}^{(I)}$	r
16	3,584	8.84e-02	7.58108e-01		7.22029e-01	
32	14,336	4.42e-02	3.93515e-01	0.95	3.58341e-01	1.01
64	57,344	2.21e-02	2.04706e-01	0.94	1.86657e-01	0.94
128	229,376	1.10e-02	1.06968e-01	0.94	9.95828e-02	0.91
256	917,504	5.52e-03	5.60719e-02	0.93	5.35364e-02	0.90

Table 16: Mesh (I) WBCR method, $\eta = \frac{1}{8\sqrt{2}}$, $\delta = \frac{1}{128}$

N	$\#N_p$	h	$E_{u_h}^{(I)}$	r	$E_{p_h}^{(I)}$	r
16	3,584	8.84e-02	1.26704		1.75263	
32	14,336	4.42e-02	7.05425e-01	0.84	9.54909e-01	0.88
64	57,344	2.21e-02	3.61245e-01	0.97	5.12135e-01	0.90
128	229,376	1.10e-02	1.81656e-01	0.99	2.60500e-01	0.98
256	917,504	5.52e-03	9.09561e-02	1.00	1.30634e-01	1.00

Table 17: Mesh (II) WBCR method, $\eta = \frac{1}{8\sqrt{2}}$, $\delta = \frac{1}{128}$

N	$\#N_p$	h	$E_{u_h}^{(II)}$	r	$E_{p_h}^{(II)}$	r
16	3,584	1.30e-01	9.89743e-01		1.02200	
32	14,336	6.39e-02	5.02759e-01	0.98	4.96331e-01	1.04
64	57,344	3.14e-02	2.53831e-01	0.99	2.53006e-01	0.97
128	229,376	1.54e-02	1.28052e-01	0.99	1.31165e-01	0.95
256	917,504	7.55e-03	6.47475e-02	0.98	6.84384e-02	0.94

Table 18: Mesh (I) WBCR method, $\eta = \frac{1}{16}$, $\delta = \frac{1}{256}$

N	$\#N_p$	h	$E_{u_h}^{(I)}$	r	$E_{p_h}^{(I)}$	r
16	3,584	8.84e-02	1.56033		2.05430	
32	14,336	4.42e-02	9.44351e-01	0.72	1.20348	0.77
64	57,344	2.21e-02	4.91889e-01	0.94	8.06744e-01	0.58
128	229,376	1.10e-02	2.48251e-01	0.99	4.77567e-01	0.76
256	917,504	5.52e-03	1.24408e-01	1.00	2.49727e-01	0.94

5 Concluding remarks

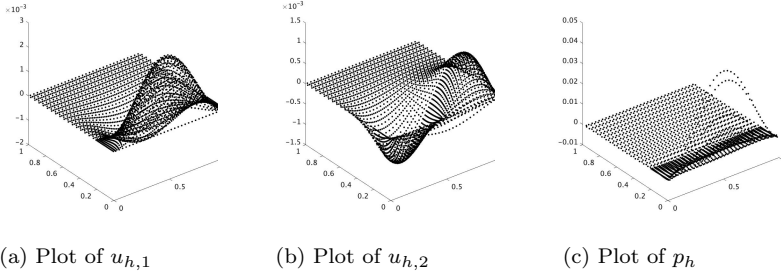
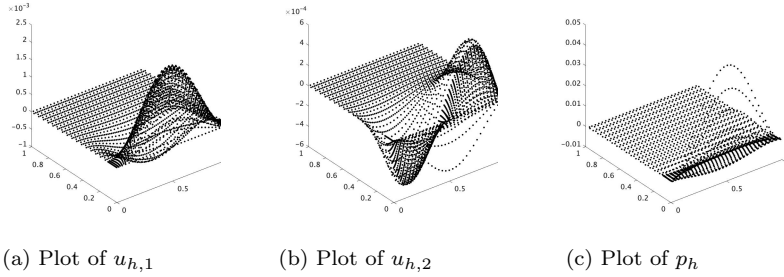
In conclusion, we identify several topics related to the results described in this work.

5.1 Discrete Poincaré and Sobolev inequalities

The discrete Poincaré and Sobolev inequalities play important roles in finite element analysis. However, to the best of our knowledge, the derivation of those inequalities remains an open question in nonconforming finite element methods on anisotropic meshes, although those inequalities are derived in [45] on shape-regular meshes. In this article, we have derived the discrete Poincaré

Table 19: Mesh (II) WBCR method, $\eta = \frac{1}{16}$, $\delta = \frac{1}{256}$

N	$\#N_p$	h	$E_{u_h}^{(II)}$	r	$E_{p_h}^{(II)}$	r
16	3,584	1.35e-01	1.32981		1.78771	
32	14,336	6.69e-02	6.72574e-01	0.98	7.85551e-01	1.19
64	57,344	3.31e-02	3.38546e-01	0.99	3.83474e-01	1.03
128	229,376	1.64e-02	1.69928e-01	0.99	1.93935e-01	0.98
256	917,504	8.13e-03	8.51702e-02	1.00	9.87999e-02	0.97

Fig. 6: Mesh (II) Plot of the WOPSIP solution, $\eta = \frac{1}{8}$, $\delta = \frac{1}{64}$ Fig. 7: Mesh (II) Plot of the WOPSIP solution, $\eta = \frac{1}{8\sqrt{2}}$, $\delta = \frac{1}{128}$

inequality by imposing that Ω is convex. Because we used the regularity of the solution of the dual problem, the convexity can be not violated in our method. In [13], the discrete Poincaré inequalities for piecewise H^1 functions are proposed. However, the inverse, trace inequalities and the local quasi-uniformity for meshes under the shape-regular condition are used for the proof. Therefore, careful consideration of the results used in [13] may be necessary to remove the assumption that Ω is convex. For example, it may be necessary to assume the minimum angle condition for simplices within macro elements. We leave further investigation of this problem as a topic for future work.

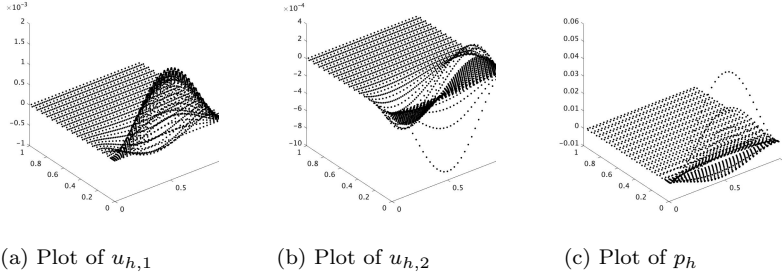


Fig. 8: Mesh (II) Plot of the WOPSIP solution, $\eta = \frac{1}{16}$, $\delta = \frac{1}{256}$

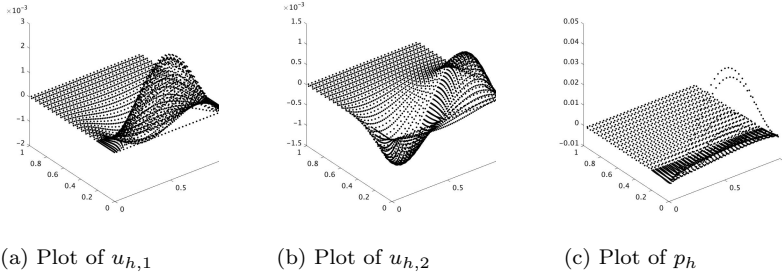


Fig. 9: Mesh (II) Plot of the WBCR solution, $\eta = \frac{1}{8}$, $\delta = \frac{1}{64}$

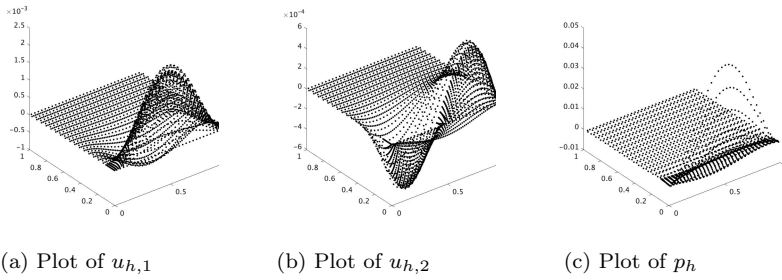


Fig. 10: Mesh (II) Plot of the WBCR solution, $\eta = \frac{1}{8\sqrt{2}}$, $\delta = \frac{1}{128}$

5.2 Advantages of the WOPSIP method

The dG scheme based on the WOPSIP method has advantages on anisotropic mesh partitions. One key advantage of the WOPSIP method is that it does not require any penalty parameter tuning. The Stokes element proposed in (2.25) satisfies the inf-sup condition. Another advantage of the method is that the error analysis of the technique is studied on more general meshes ([16, 15, 14,

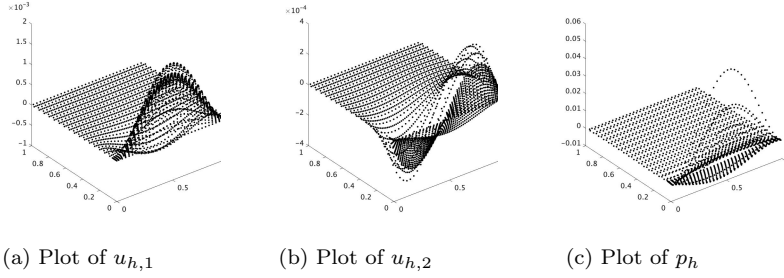


Fig. 11: Mesh (II) Plot of the WBCR solution, $\eta = \frac{1}{16}$, $\delta = \frac{1}{256}$

8]) than conformal meshes. This enables meshes with hanging nodes, whereas handling those meshes in the classical CR nonconforming finite element might be difficult. Here, we briefly treat the WOPSIP method on nonconforming meshes in our framework.

Let $d = 2$. According to [14, Section 2.7], a nonconforming \mathbb{T}_h on Ω is defined as satisfying the following condition:

- If an edge of $T \in \mathbb{T}_h$ contains hanging nodes, it is the union of the edges of other triangles in \mathbb{T}_h .

The definition of the set \mathcal{F}_h^i in Section 2.3 is modified as follows: An (open) interior edge of a triangle in \mathbb{T}_h belongs to \mathcal{F}_h^i if and only if

- (I) it is the common edge of exactly two triangles, or
- (II) it contains a hanging node.

An excellent feature of the WOPSIP method for nonconforming is that the CR interpolation defined in (2.26) is unaffected by the hanging nodes; that is, the relations (3.16) and (3.24) remain valid. Therefore, if the relation (3.7) holds, then the error estimates in Theorem 3.7 may provide coverage as $h \rightarrow 0$ for nonconforming meshes. We leave further investigation of the hanging nodes for future work.

Acknowledgements We also thank the anonymous referees for their valuable comments and suggestions.

Data Availability

Data supporting the findings of this study are available from the corresponding author upon request.

Conflict of interest

The authors declare no conflicts of interest associated with this manuscript.

References

1. Acosta, G., Apel, Th., Durán, R.G., Lombardi, A.L.: Error estimates for Raviart–Thomas interpolation of any order on anisotropic tetrahedra, *Mathematics of Computation* **80** No. 273, 141-163 (2010)
2. Acosta, G., Durán, R.G.: The maximum angle condition for mixed and nonconforming elements: Application to the Stokes equations, *SIAM J. Numer. Anal.* **37**, 18-36 (1999)
3. Apel Th, Nicaise S, Schöberl J: Crouzeix–Raviart type finite elements on anisotropic meshes. *Numer Math* **89**, 193-223 (2001)
4. Andreas W. Stabilised mixed finite-element methods on anisotropic meshes. PhD thesis: University of Strathclyde (2015)
5. Apel, T. Anisotropic finite elements: local estimates and applications. *Advances in Numerical Mathematics*. Teubner & Stuttgart (1999)
6. Apel, T., Kempf V., Linke, A. and Merdon, C.. Non-conforming pressure-robust finite element method for Stokes equations on anisotropic meshes. *IMA J. Numer. Anal.*, (2021)
7. Babuška, I. Aziz, A. K.: On the angle condition in finite element method. *SIAM J. Numer. Anal.* **13**, 214-226 (1976)
8. Barker, A. T., Brenner, S. C.: A mixed finite element method for the Stokes equations based on a weakly overpenalized symmetric interior penalty approach. *J. Sci. Comput.* **58**, 290-307 (2014)
9. Barrenechea, G. R., Wachtel, A.: The inflow stability of the lowest-order Taylor–Hood pair on affine anisotropic meshes. *IMA J. Numer. Anal.* **40**, 2377-2398 (2019)
10. Boffi, D., Brezzi, F., Demkowicz, L.F., Durán, R.G., Falk, R.S., Fortin, M.: *Mixed Finite Elements, Compatibility Conditions, and Applications: Lectures Given at the C.I.M.E. Summer School, Italy, 2006*. *Lunk Notes in Mathematics* **1939** and Springer (2008)
11. Boffi, D., Brezzi, F., Fortin, M.: *Mixed Finite Element Methods and Applications*. Springer-Verlag, New York (2013).
12. Brandts, J., Korotov, S. & Krížek, M.: On the equivalence of regularity criteria for triangular and tetrahedral finite-element partitions. *Comput. Math, Appl.* **55**, 2227–2233 (2008)
13. Brenner, S. C.: Poincaré–Friedrichs inequalities for piecewise H^1 functions. *SIAM J. Numer. Anal.* **41** (1), 306-324 (2003)
14. Brenner, S. C. Forty years of the Crouzeix–Raviart element. *Numer. Methods Partial Differential Equations* **31**, 367-396 (2015)
15. Brenner, S. C., Owens, L., Sung, L. Y., A weakly over-penalised symmetric interior penalty method. *Electron. Trans. Numer. Anal.* **30**, 107-127 (2008)
16. Brenner, S. C., Owens, L., Sung, L. Y.: Higher-order weakly overpenalized symmetric interior penalty methods. *J. Comput. App. Math* **236**, 2883-2894 (2012)
17. Brenner, S. C., Scott, L. R.: *The Mathematical Theory of Finite Element Methods*. Springer-Verlag, New York (2008).
18. Chen, S., Liu, M., Qiao, Z. Anisotropic nonconforming element for fourth-order elliptic singular perturbation problem. *International Journal of Numerical Analysis and Modeling* **7** (4), 766-784 (2010)
19. Crouzeix, M., Raviart, P.-A.: Conforming and nonconforming finite element methods for solving stationary Stokes equations, I. *RAIRO Anal. Numér.* **7**, 33-76 (1973)
20. Dong Z., Georgoulis E.. Robust interior penalty discontinuous Galerkin methods. *J. Sci. Comput.* **92**, (2022)
21. Egger, H., Waluga, C.: hp Analysis of a hybrid DG method for Stokes flow, *IMA J. Numer. Anal.*, **33**, 687-721 (2013)
22. Ern, A., Guermond, J.L.: *Theory and Practice of Finite Elements*. Springer-Verlag, New York (2004).
23. Ern, A., Guermond, J.L.: *Finite Elements I: Approximation and Interpolation*. Springer-Verlag, New York (2021).
24. Ern, A. and Guermond, J. L.: *Finite elements II: Galerkin Approximation, Elliptic and Mixed PDEs*. Springer-Verlag, New York (2021).
25. Ern, A. and Guermond, J. L.: *Finite elements III: First-Order and Time-Dependent PDEs*. Springer-Verlag, New York (2021).

26. Fortin M. Analysis of the convergence of mixed finite element methods. *RAIRO Anal. Numér.* **11**, 341-354 (1977)
27. Girault, V. and Raviart, P. A. Finite element methods for Navier-Stokes equations. Springer-Verlag-Verlag (1986).
28. Grisvard, P. Elliptical problems in Nonsmooth domains. SIAM, (2011)
29. Hecht, F.: FREEFEM Documentation, Finite element. <https://doc.freefem.org/documentation/finite-element.html>
30. Hecht, F.: <http://www.um.es/freefem/ff++/uploads/Main/LapDG2.edp>, (2003)
31. Hecht, F., Pironneau, O., Morice, J., Hyaric, A. L., Ohtsuka, K. & FreeFem++ version 4.90. <https://freefem.org>, (2012)
32. Ishizaka H. Anisotropic interpolation error analysis using a new geometric parameter and its applications. Ehime University, Ph. D. thesis (2022).
33. Ishizaka and H. Anisotropic Raviart–Thomas interpolation error estimates using a new geometric parameter. *Calcolo* **59**, (4) and (2022).
34. Ishizaka, H., Kobayashi, K., Tsuchiya, T.: General theory of interpolation error estimates on anisotropic meshes. *Jpn. J. Ind. Appl. Math.*, **38** (1), 163-191 (2021)
35. Ishizaka, H., Kobayashi, K., Tsuchiya, T.: Crouzeix–Raviart and Raviart–Thomas finite element error analysis on anisotropic meshes violating the maximum angle condition. *Jpn. J. Ind. Appl. Math.*, **38** (2), 645-675 (2021)
36. Ishizaka, H., Kobayashi, K., Suzuki, R., Tsuchiya, T.: A new geometric condition equivalent to the maximum angle condition for tetrahedrons. *Computers & Mathematics with Applications* **99**, 323-328 (2021)
37. Ishizaka H., Kobayashi K., Tsuchiya T. Anisotropic interpolation error estimates using a new geometric parameter. *Jpn. J. Ind. Appl. Math.*, **40** (1), 475-512 (2023)
38. John V. Finite element methods for incompressible flow problems. Springer (2016)
39. Kashiwabara, T., Tsuchiya, T. Robust discontinuous Galerkin scheme for anisotropic meshes. *Jpn. J. Ind. Appl. Math.*, **38**, 1001-1022 (2021)
40. Krížek, M.: maximum angle condition for linear tetrahedral elements. *SIAM J. Numer. Anal.* **29**, 513-520 (1992)
41. Kunert G. A. posteriori L2 error estimation on anisotropic tetrahedral finite element meshes. *IMA Journal of Numerical Analysis* **21** (2), 503-523 (2001)
42. Linke A: The role of Helmholtz decomposition in mixed methods for incompressible flows and a new variational crime. *Comput. Methods Anall. Mech. Engrg.* **268**, 782-800 (2014)
43. Linß, T. Layer-adapted meshes for reaction vector diffusion problems. Springer (2010)
44. Oikawa, I., Kikuchi, F.: From FEM to Discontinuous Galerkin Methods (4) Applications of the HDG Method. *Bulletin of the Japan Society for Industrial and Applied Mathematics* **27** (4), 33-38 (2017) https://www.jstage.jst.go.jp/article/bjsiam/27/4/27_33/_article/-char/en
45. Di Pietro, D. A., Ern, A., Mathematical aspects of discontinuous Galerkin methods. Springer-Verlag (2012)
46. Di Pietro, D. A., Ern, A., Linke, A. & Schieweck, F.: A discontinuous skeletal method for the viscosity-dependent Stokes problem. *Computer Methods in Applied Mechanics and Engineering*, 175-195 (2016)
47. Rivière, B.: Discontinuous Galerkin Methods for Solving Elliptic and Parabolic Equations. SIAM, (2008)
48. Roos, H.G., Stynes, M., Tobiska, L.: Robust numerical methods for Singularly Perturbed differential equations. Springer-Verlag, Berlin, Heidelberg (2008)
49. Sohr, H.: The Navier-Stokes Equations: An Elementary Functional Analytic Approach. Birkhä User, Boston, Basel, Berlin (2001)